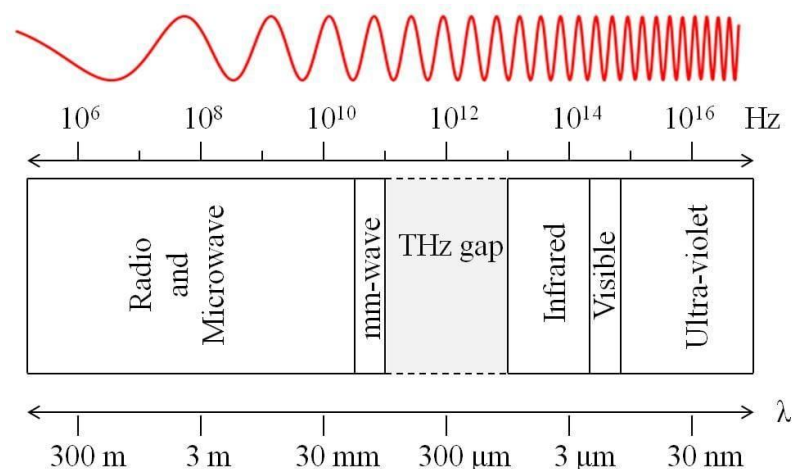


Development of Superconducting Single-Photon Detectors for Quantum Information Applications

Adriana E. Lita
NIST Boulder

A single-photon detector is a device that is able to produce a measurable output signal, distinguishable from noise, due to a **single photon** incident on the detector's input plane

Single-Photon Sources and Detectors Dictionary
<https://doi.org/10.6028/NIST.IR.8486r1>



$$\lambda = 1550 \text{ nm}$$
$$E_{\text{ph}} = hc/\lambda = 1.3 \cdot 10^{-19} \text{ J}$$

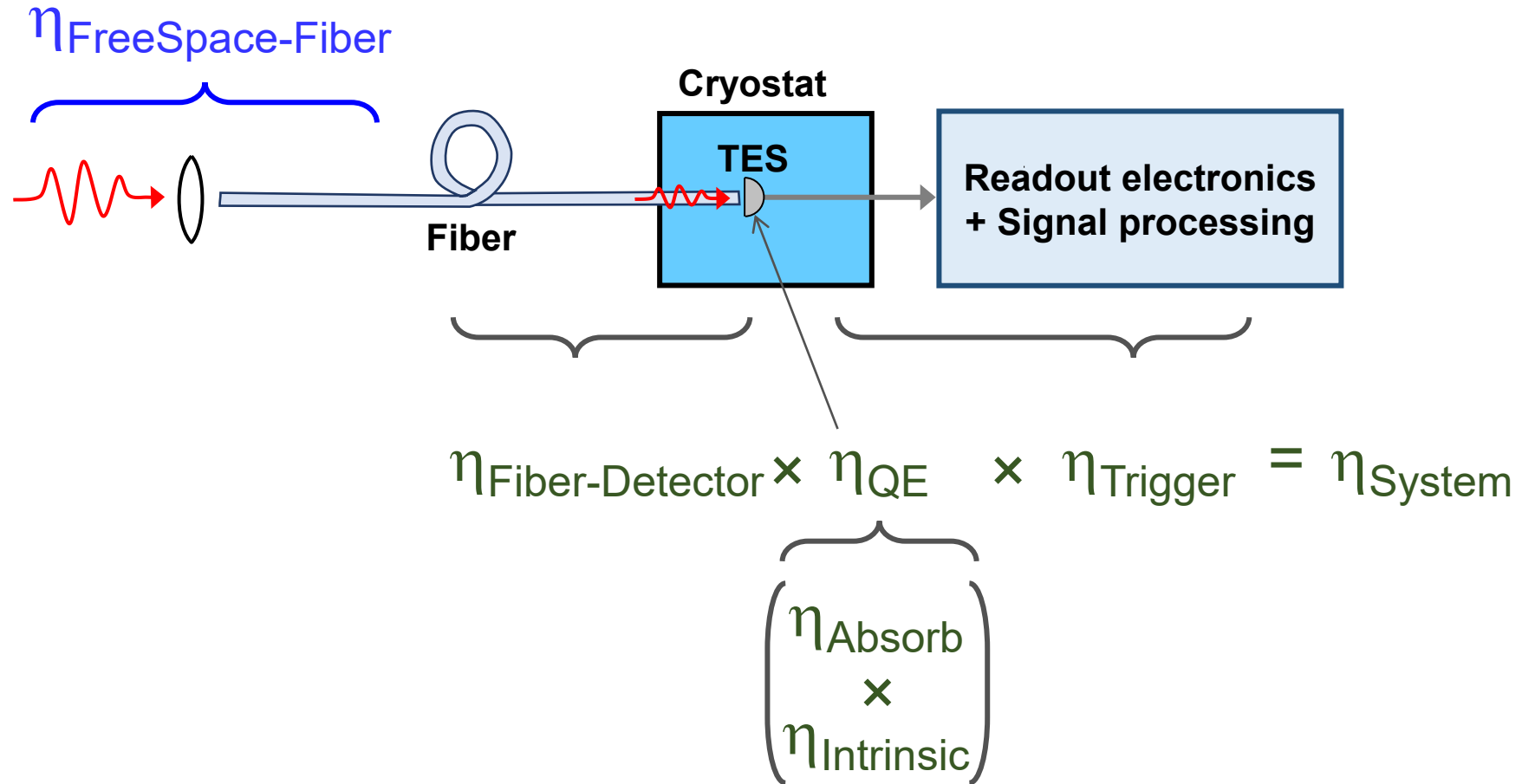
Single-Photon Detector Performance metrics

- System Detection Efficiency (SDE)
- Energy Resolution/Photon-Number Resolution (PNR)
- Timing jitter
- Recovery time (Count Rate)
- Dark/Background count rate (DCR)
- Tunable wavelength

Other considerations

- Operating Temperature
- Scalability (multi-pixel arrays, low readout-circuit complexity)

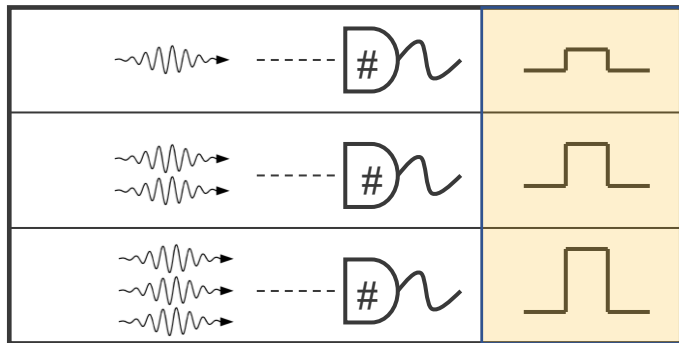
System Detection Efficiency (SDE)



Photon-number resolving (PNR)

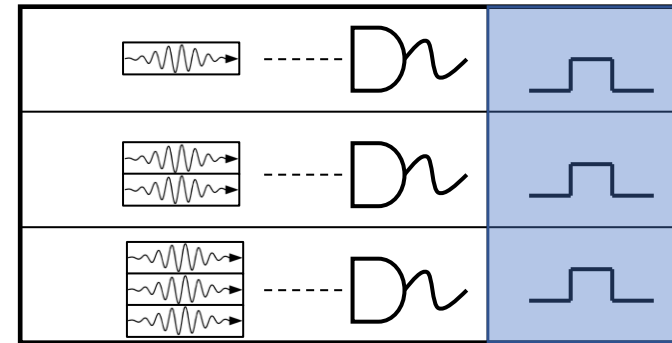
Photon Number Resolving

Output signal proportional to photon number



Conventional (Click Detector)

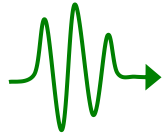
Same output signal for varying photon number input



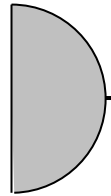
Timing Jitter

Timing jitter is a measure of the variation in detector latency

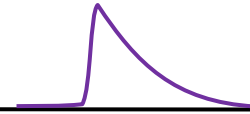
Single photon



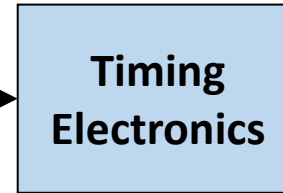
Single-Photon Detector



Electrical Pulse

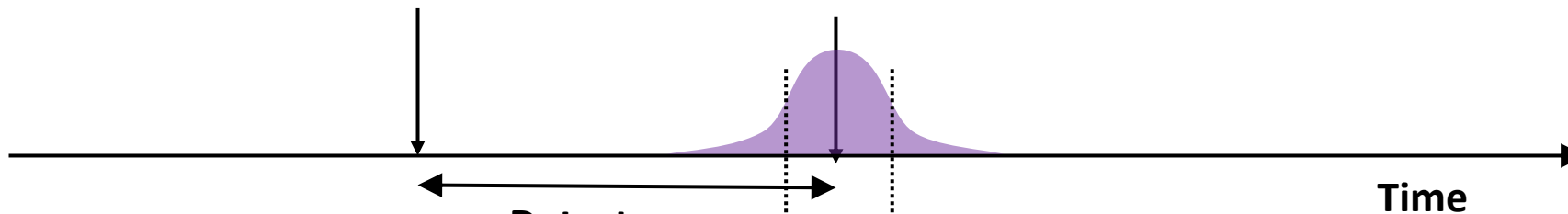


Timing Electronics



Photon arrives at detector

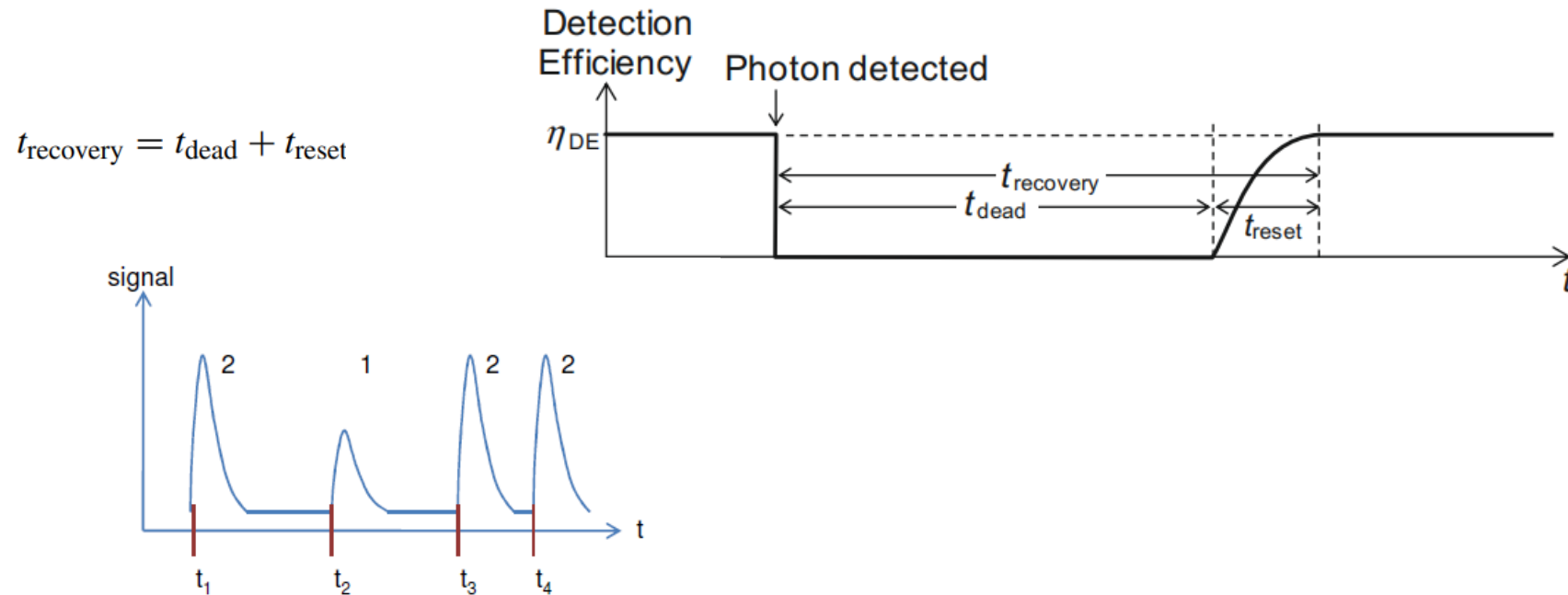
Electrical pulse exits detector



- Uncertainty in determining the photon arrival time
- Depends on rise time, pulse size, amplitude noise, bandwidth of electronics

Recovery Time (Count Rate)

- Time it takes the detector to be ready to count the next event
- Sets a limit on the maximum count rate
- For a strongly asymmetric pulse defined as the $1/e$ time constant of the recovery
- Ideally want recovery times within source repetition rate



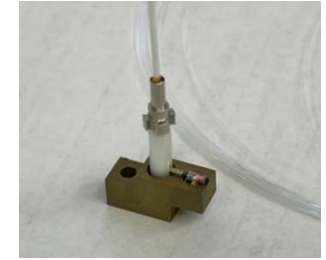
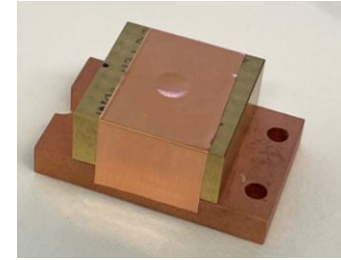
Dark Counts and Background Counts

Dark Counts:

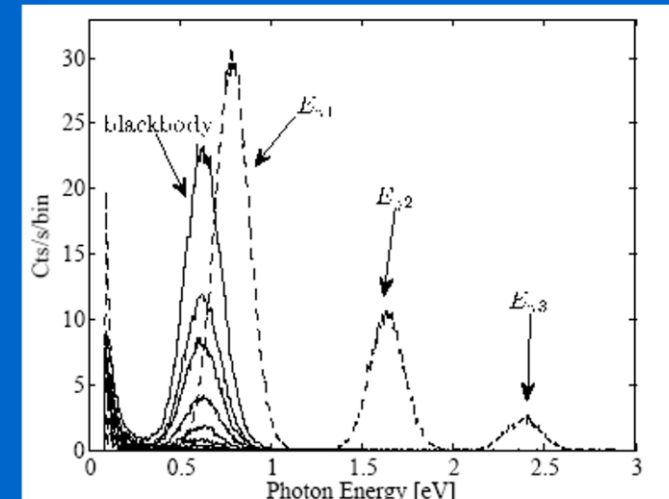
- False registering of a photon triggered by electrical or thermal fluctuations (detector operating principle)
 - Tunneling effects, afterpulsing, material defects
 - cosmic rays energy depositions, ambient radioactivity, quantum fluctuations
- **< 1 cnt/day for superconducting SPD**

Background Counts:

- Due to unwanted photons, not noise/fluctuation
 - Photons from blackbody radiation from room temperature objects can propagate down the optical fiber, creating a background count rate.
 - External light



Histogram of detected 1550 nm photons
Blackbody photons 0°C to 70°C.



A.J. Miller et al. Proc. of the 8th Int. Conf. Quantum
Comm. Meas. Comp, 445 (2007)

Photomultiplier Tube



PMT

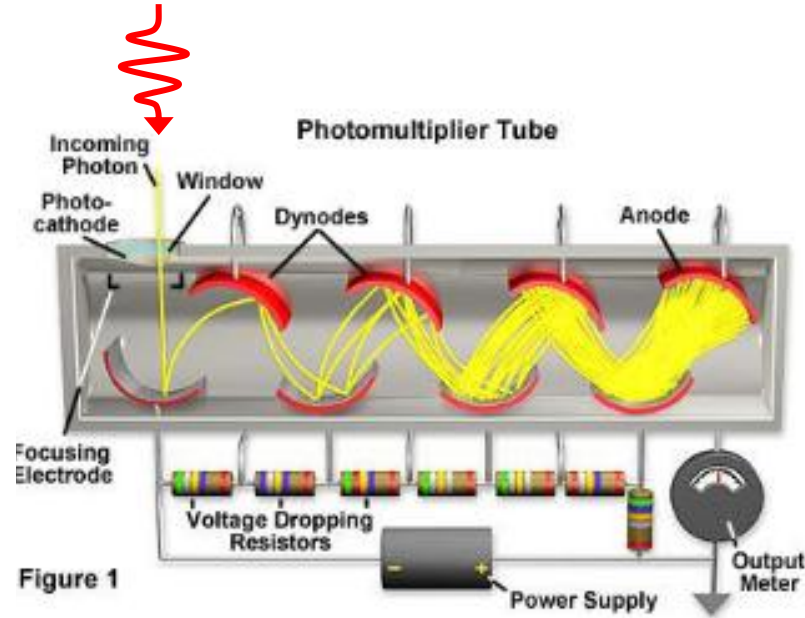
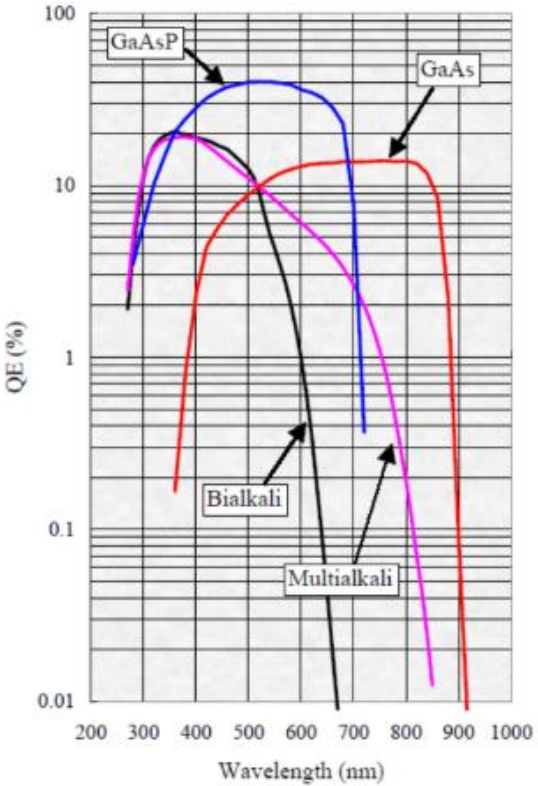


Figure 1

- Oldest SPD technology
- Works best in the UV/blue
- Large area devices (> 8 mm diam)

Efficiency	≤ 40 %
Energy Resolution	Yes
Recovery Time	50 ns
Timing Jitter	50 ps
Dark Counts	< 200 cps
Wavelength Range	UV-VIS
Operating Temperature	RT

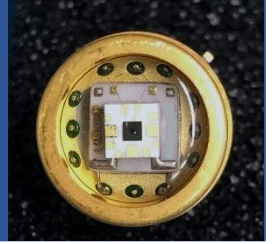


courtesy K. Dhimitri, Hamamatsu

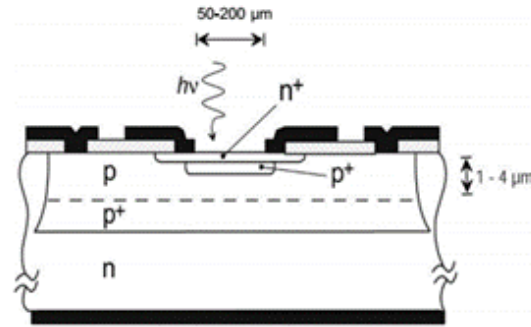
- Applications: Spectrophotometers; Medical diagnosis; Environmental measurements; LIDAR; High Energy Physics

Single-Photon Avalanche Photodiode

SPAD

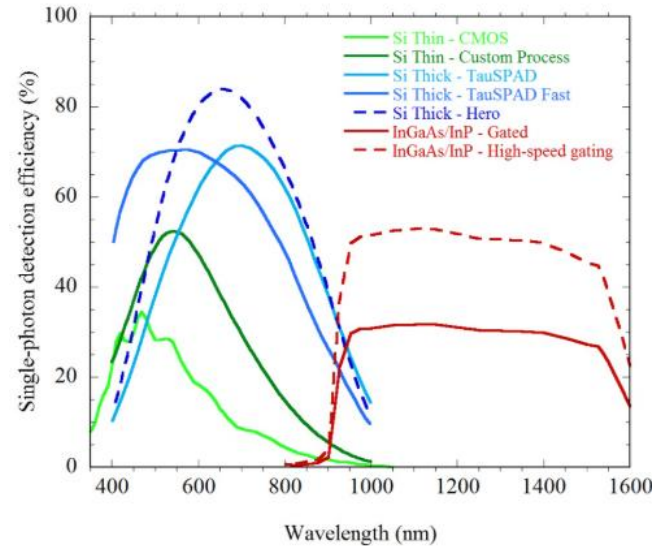


Thin Si SPAD (Planar structure)



Typical active area diameter: 50-200 μm
1 μm thick

lower jitter (10's of ps)
lower detection efficiency



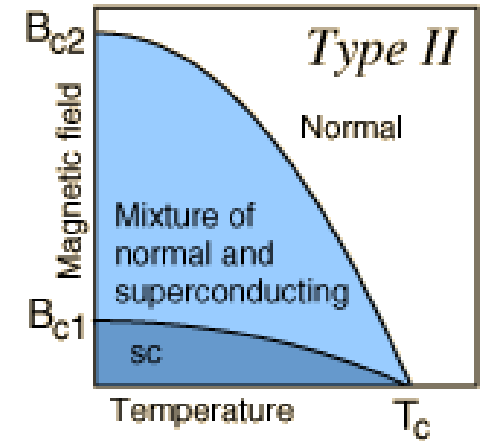
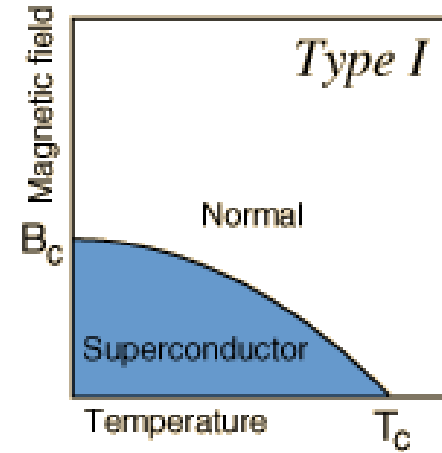
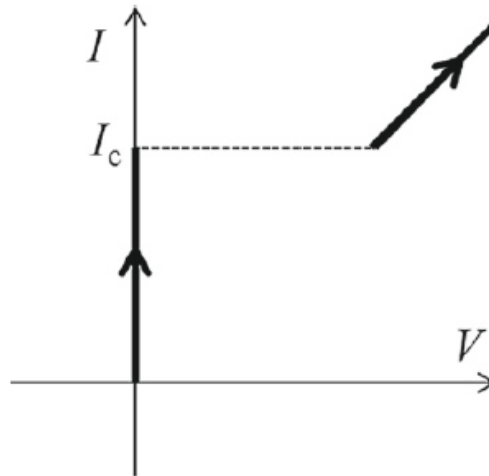
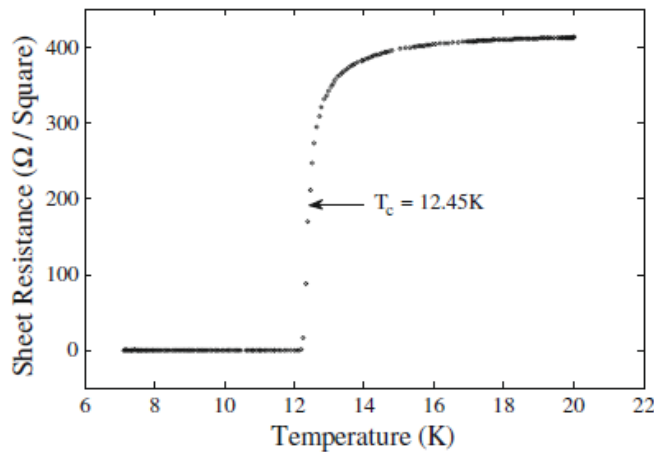
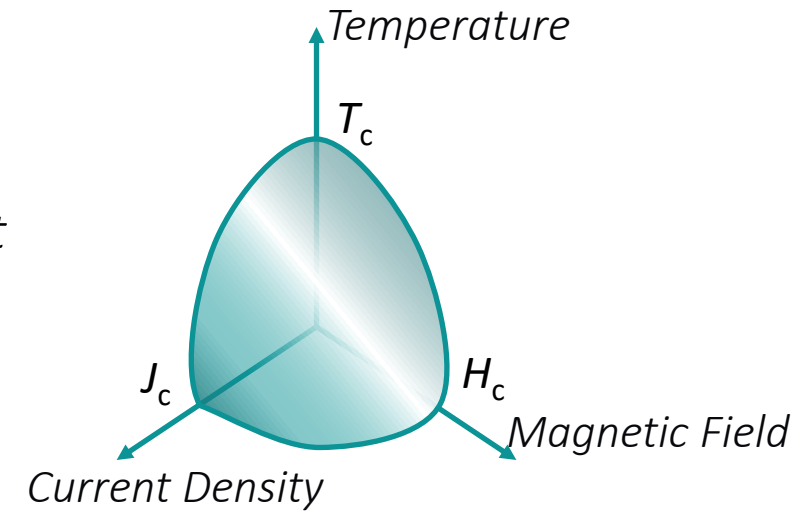
courtesy J. Bienfang, NIST

Efficiency	85 %
Energy Resolution	Some
Recovery Time	10 ns
Timing Jitter	20 ps
Dark Counts	< 100 cps
Wavelength Range	UV-NIR
Operating Temperature	RT

Applications: Quantum Computing: QKD; Quantum Optics; 3D Imaging, ToF Imagers; LIDAR; Biomedical Imaging

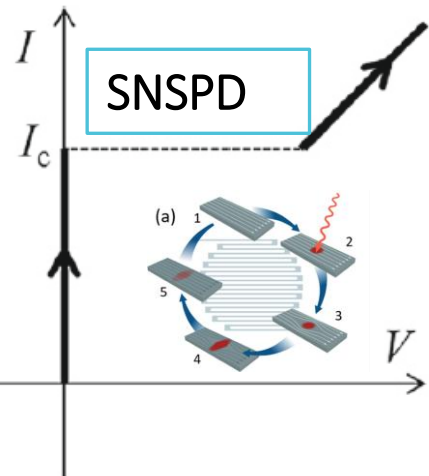
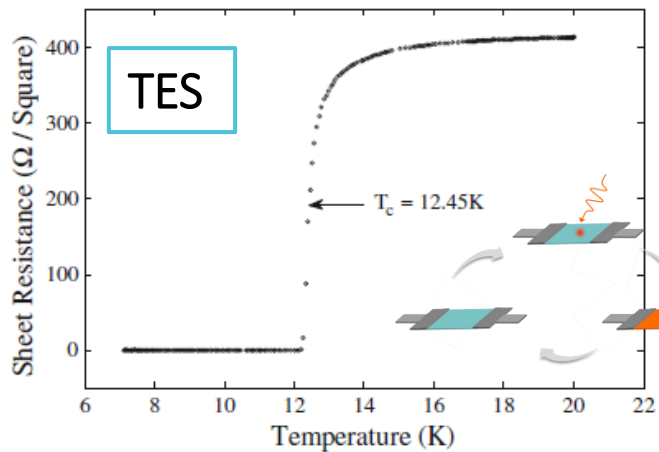
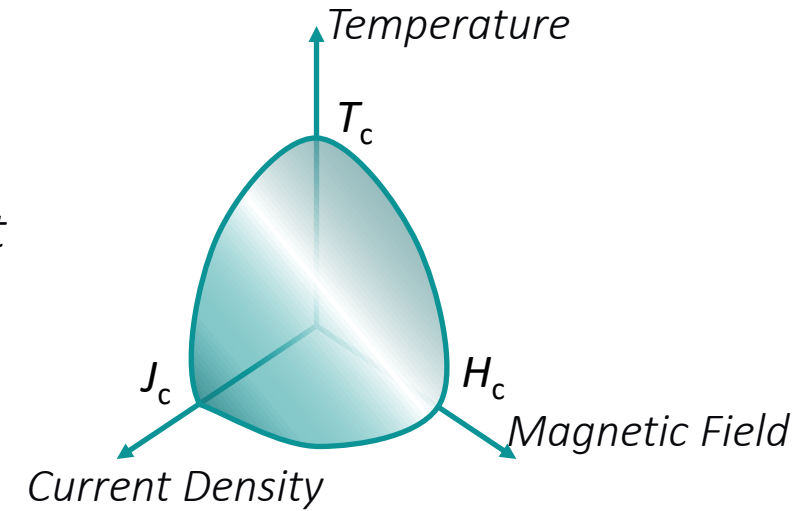
Superconductivity

- Distinct thermodynamic phase observed only in some solids
- Exists only when the *Temperature*, external *Magnetic Field*, and the *Current Density* carried by the material are below critical values (T_c , H_c and J_c)
 - Ground State = Cooper pairs
 - Excited State = quasi-particles
 - Energy Gap $2\Delta = 3.528 K_B T_c$ (meV)

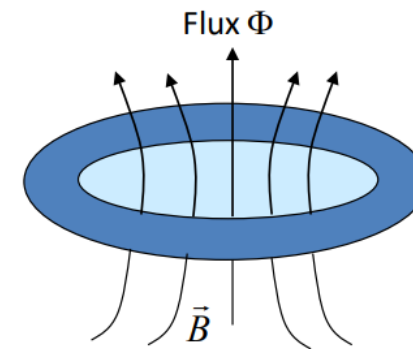


Superconductivity

- Distinct thermodynamic phase observed only in some solids
- Exists only when the *Temperature*, external *Magnetic Field*, and the *Current Density* carried by the material are below critical values (T_c , H_c and J_c)
 - Ground State = Cooper pairs
 - Excited State = quasi-particles
 - Energy Gap $2\Delta = 3.528 K_B T_c$ (meV)



Macroscopic Quantum Effects

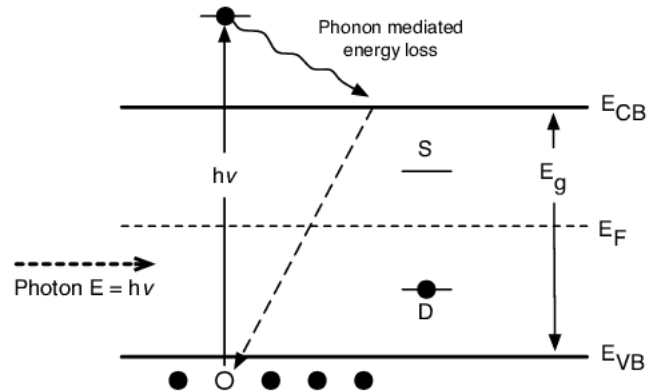


$$\Phi_0 = \frac{2\pi\hbar c}{q} = \frac{hc}{q}$$

Flux quantization $\Phi = n\Phi_0$
Josephson Effects

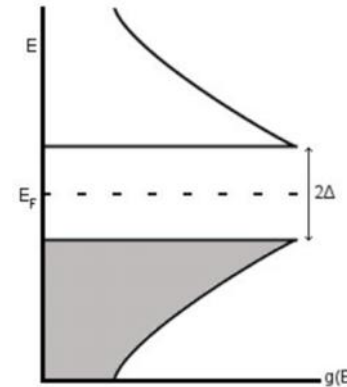
Why Superconducting Detectors?

- Superconducting detectors are the lowest noise, highest sensitivity detectors available
- They require cryogenic operation (0.05 K – 4 K).



Semiconductor Bandgap

- Si 1.12 eV
- InGaAs 0.75 eV

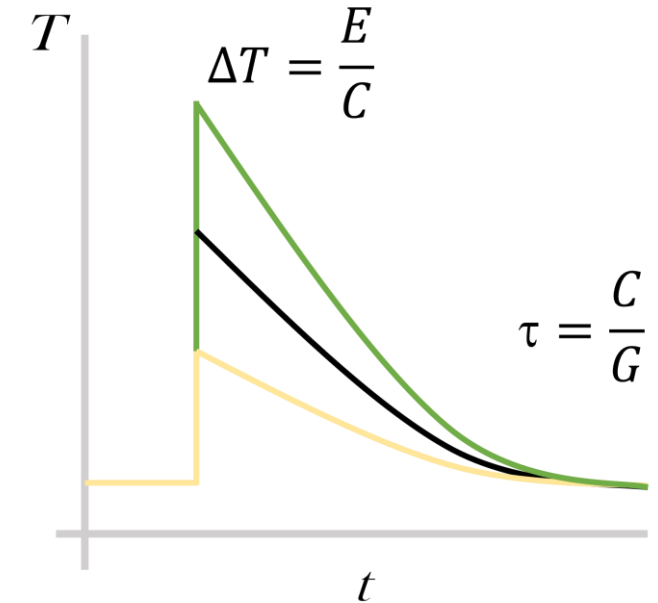
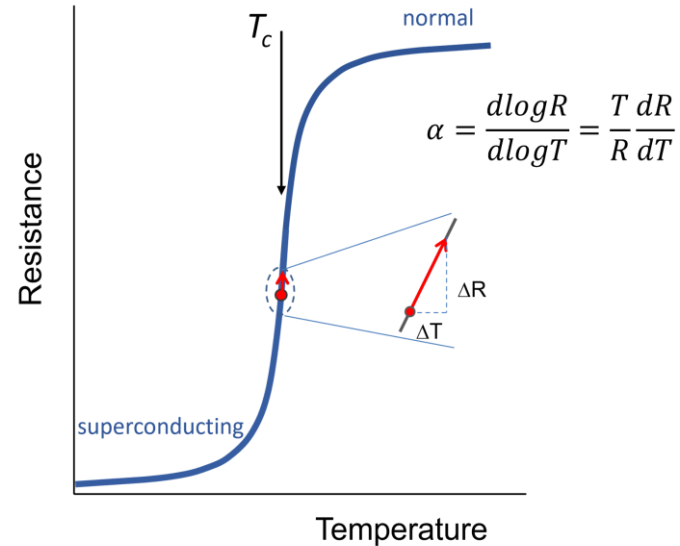
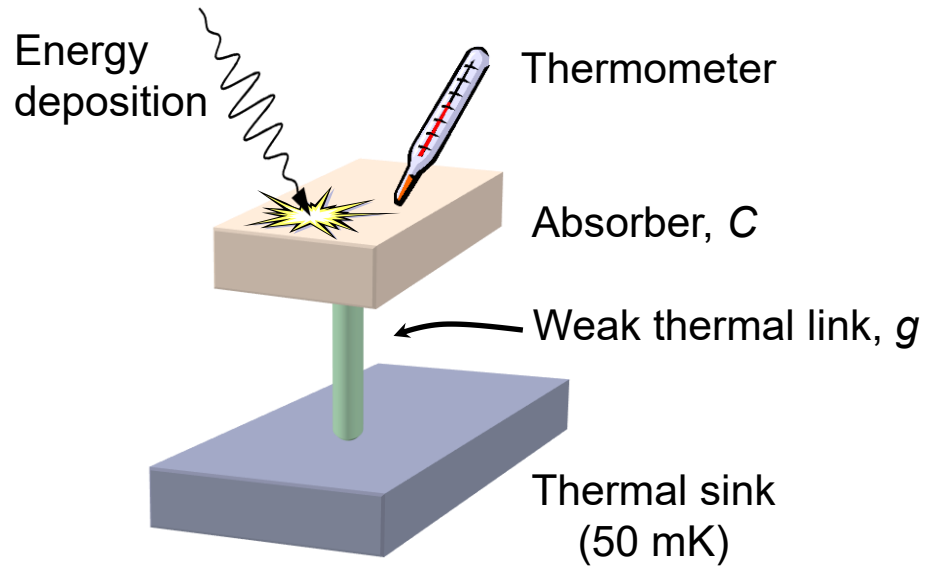


Superconducting Gap Energy

- Nb 2.32 meV
- Al 0.34 meV

Transition-Edge Sensors (TES)

C = heat capacity
 G = thermal conductance

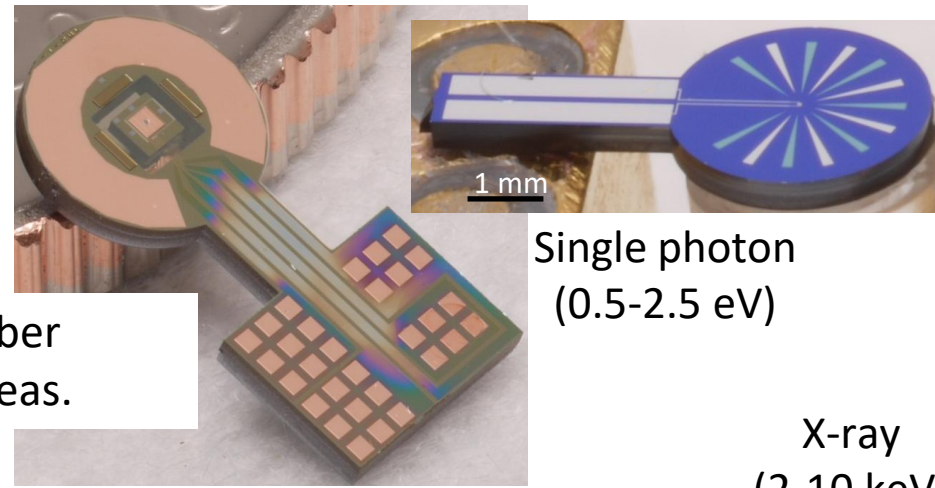
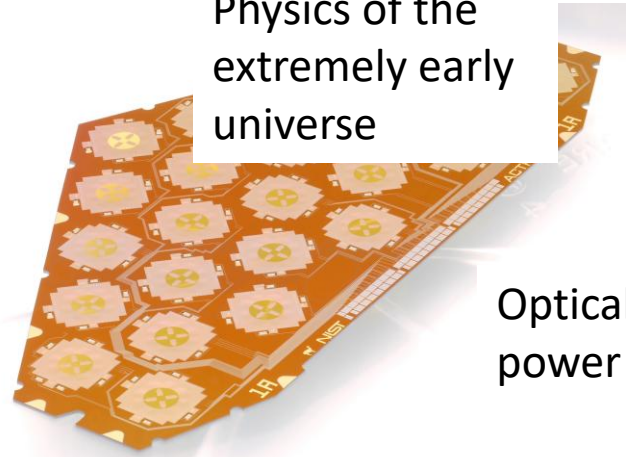


- Calorimetric principle: turn photon energy into heat and measure it
- Enables direct measurement of absorbed energy
- Operating temperature ~ 100 mK ; Thermal fluctuation noise $\Delta E \sim \sqrt{4k_B T^2 C}$

TES Devices Across the Spectrum

Quantum Information

Physics of the extremely early universe

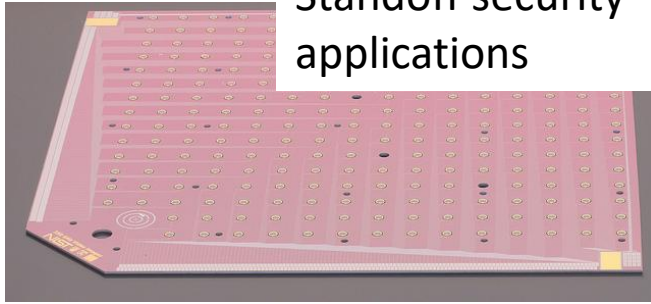


Single photon (0.5-2.5 eV)

Optical fiber power meas.

Across the Spectrum

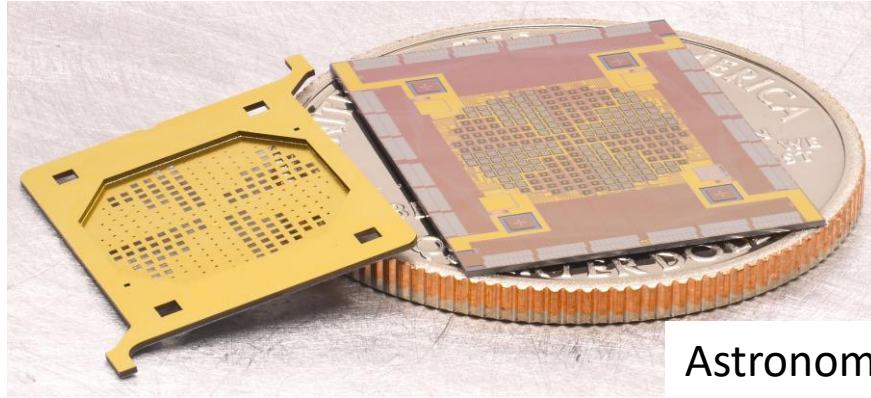
Cosmic Microwave Background (0.6 meV, 150 GHz)



THz Imaging (4 meV, 0.35 THz)

Standoff security applications

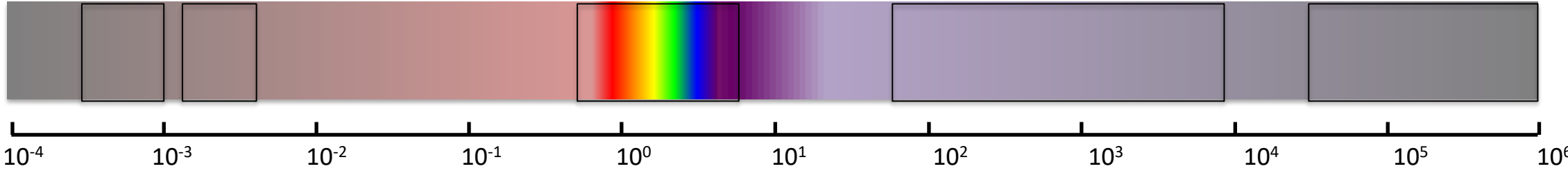
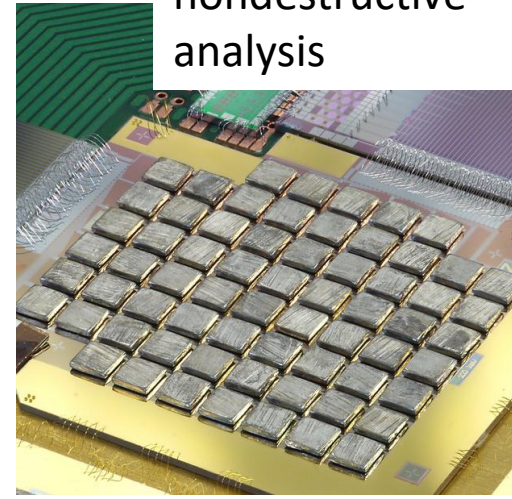
X-ray (2-10 keV)



Astronomy

Gamma-ray (100's keV)

Nuclear nondestructive analysis



Optical Transition-Edge Sensor (TES)

APPLIED PHYSICS LETTERS

VOLUME 73, NUMBER 6

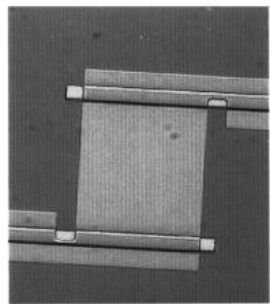
10 AUGUST 1998

Detection of single infrared, optical, and ultraviolet photons using superconducting transition edge sensors

B. Cabrera,^{a)} R. M. Clarke, P. Colling, A. J. Miller, S. Nam, and R. W. Romani
Physics Department, Stanford University, Stanford, California 94305-4060

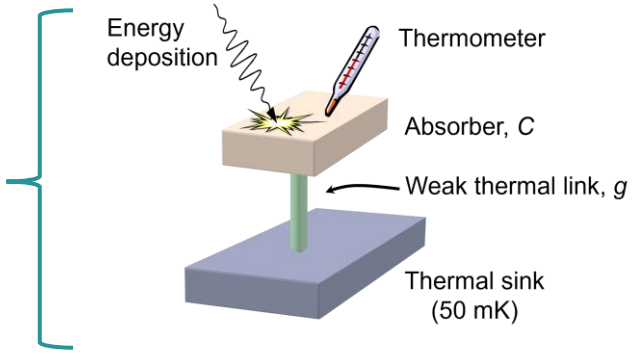
(Received 2 March 1998; accepted for publication 8 June 1998)

We have demonstrated the use of superconducting transition edge sensors for the wide-band detection of individual photons from the mid infrared (IR), through the optical, and into the far ultraviolet (UV). These tungsten transition edge sensors are squares about $18 \mu\text{m}$ on a side and detect single photon events above a threshold of 0.3 eV ($4 \mu\text{m}$ wavelength), with an energy resolution of 0.15 eV full width at half maximum, and with a risetime (falltime) of $.5 \mu\text{s}$ ($60 \mu\text{s}$). The calibration data extend up to the UV cutoff of the fiber optic feed at 3.5 eV (350 nm). © 1998 American Institute of Physics. [S0003-6951(98)03032-0]

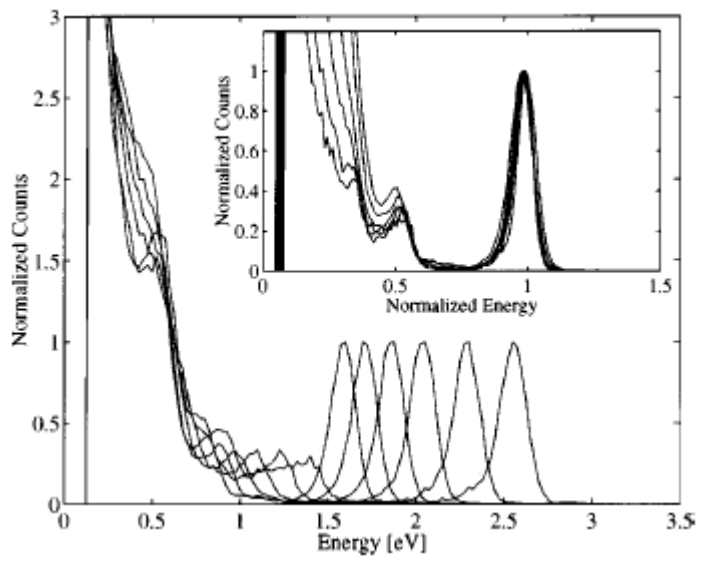


W sensor and Al voltage rails

The entire micro-calorimeter is in the superconducting film

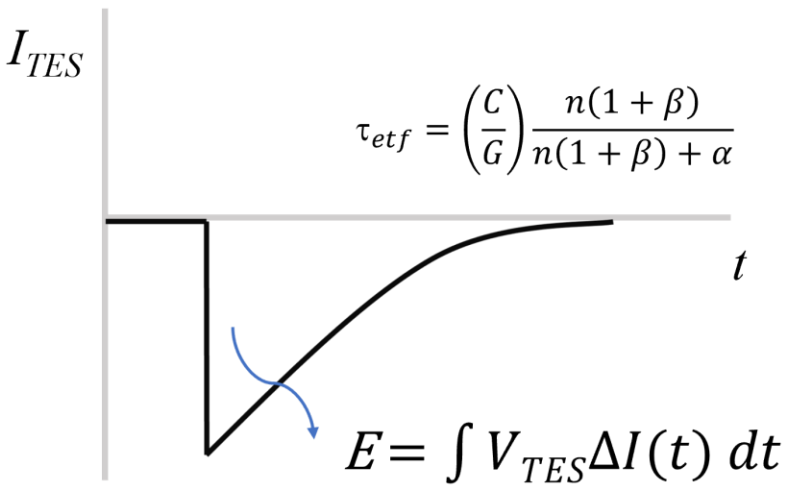
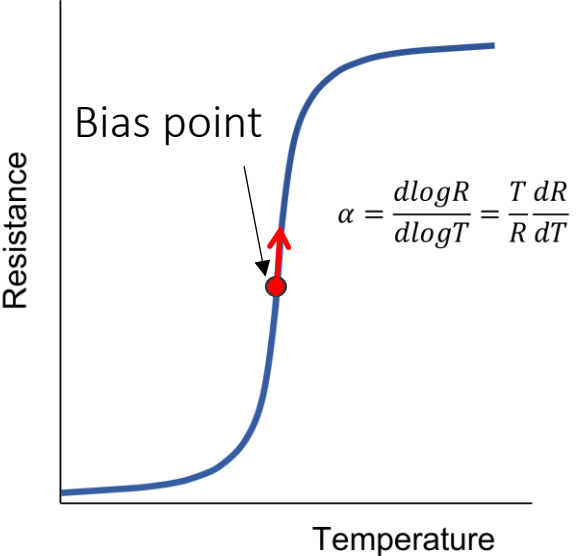
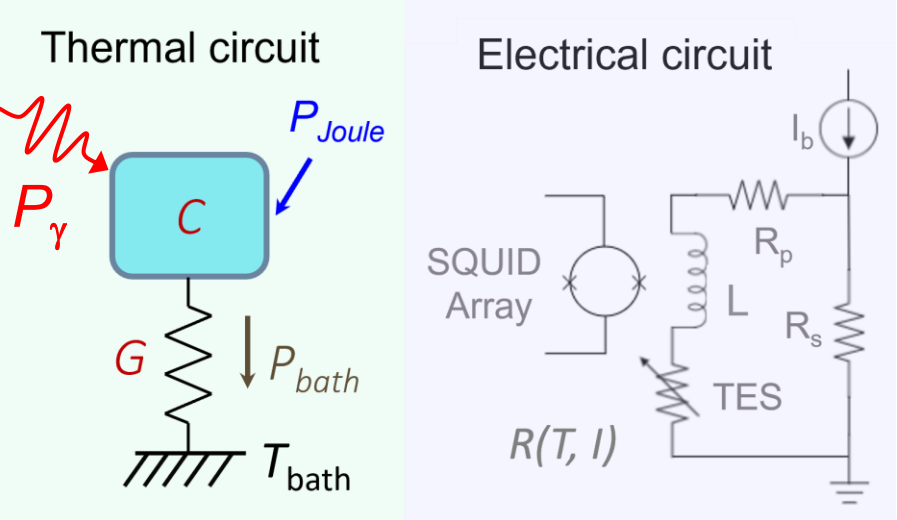
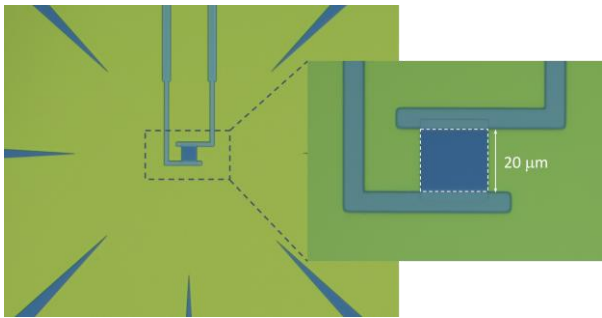


- e^- in W
- e^- in W
- e^- - ph decoupling
- phonons in W



Optical Transition-Edge Sensor (TES)

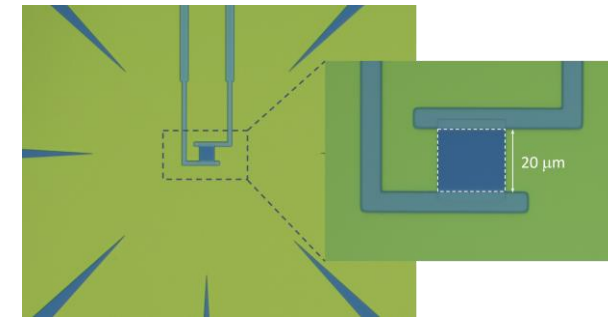
Electrical and Thermal circuit: Electrothermal Feedback



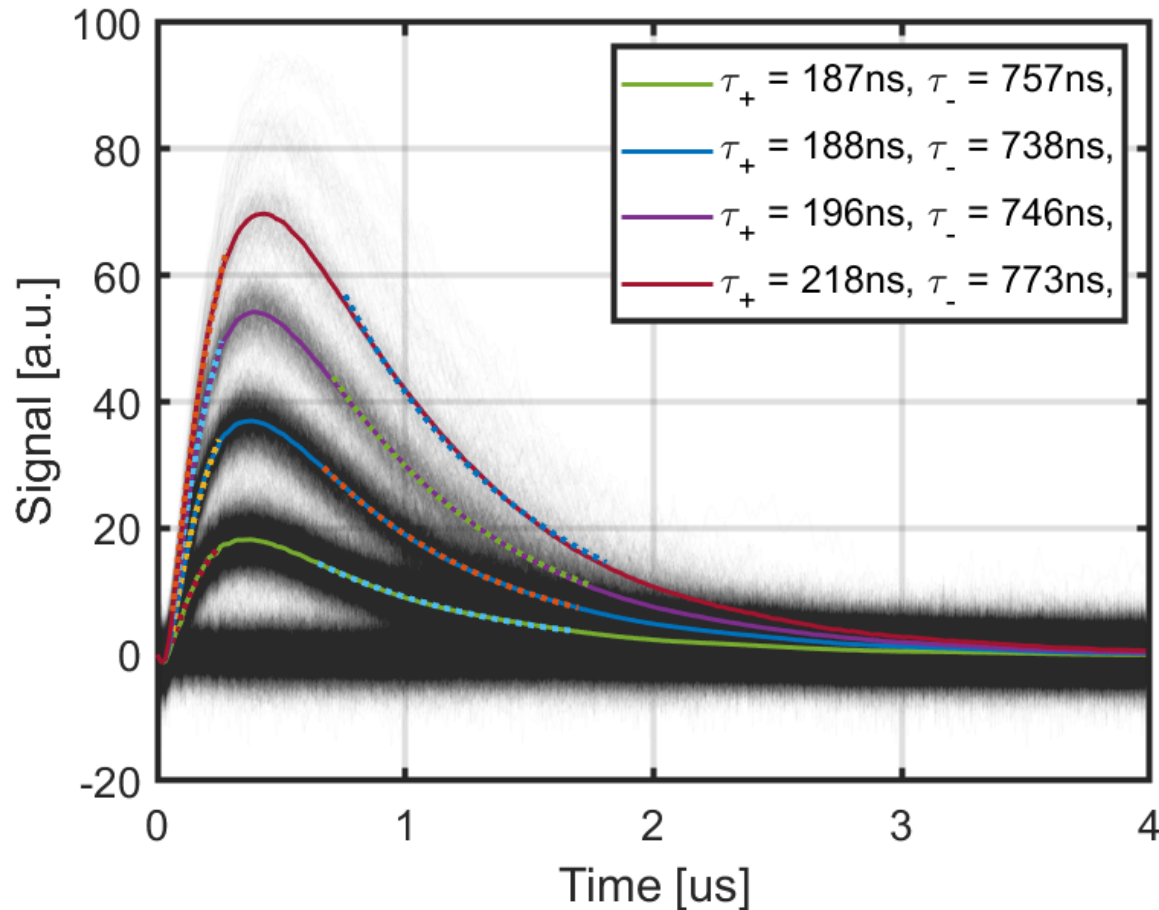
K.D. Irwin and G.C. Hilton, Cryogenic Particle Detection, Topics in Applied Physics, Vol. 99, (2005)

- Voltage bias keeps e^- in superconducting-to-normal transition via Joule heating ($R_{TES} \neq 0$)
- The heat in excess of Joule heating at equilibrium is removed through a drop in the Joule power dissipation
- Enables direct measurement of photons energy (integral of the current change * voltage bias)

Optical TES Output Signal



100,000 TES traces in response to 1550 nm pulsed laser



n=4 3.2 eV

n=3 2.4 eV

n=2 1.6 eV

n=1 0.8 eV

n=0

- Output signal is proportional to incoming photon energy
- Enables direct measurement of absorbed energy
- Rise time of ~ 100 ns
- Pulse duration $\sim 1-2$ μ s
- Essentially no Dead time
- TES materials: W, Ti, Hf, Ir, TiAu/AuTi, TiAg...

Optical Transition-Edge Sensor (TES)

APPLIED PHYSICS LETTERS

VOLUME 83, NUMBER 4

Demonstration of a low-noise near-infrared photon counter with multiphoton discrimination

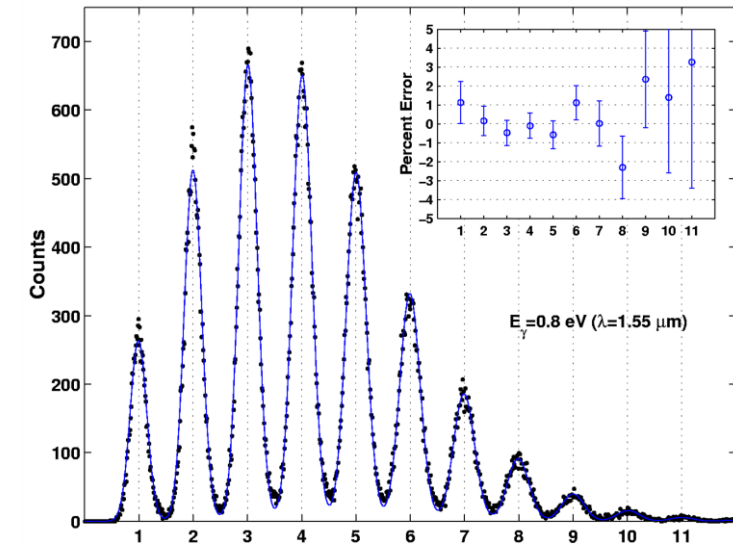
Aaron J. Miller,^{a)} Sae Woo Nam, and John M. Martinis
National Institute of Standards and Technology, 325 Broadway, Boulder, Colorado 80305

Alexander V. Sergienko
Quantum Imaging Laboratory, Boston University, 8 Saint Mary's Street, Boston, Massachusetts 02215

(Received 20 February 2003; accepted 5 June 2003)

We have demonstrated a system capable of directly measuring the photon-number state of a single pulse of light using a superconducting transition-edge sensor microcalorimeter. We verify the photon-number distribution of a weak pulsed-laser source at 1550 nm. Such single-photon

1550 nm Weak Coherent Source



PHYSICAL REVIEW A 68, 063817 (2003)

Direct observation of photon pairs at a single output port of a beam-splitter interferometer

Giovanni Di Giuseppe,^{1,*} Mete Atatüre,^{2,†} Matthew D. Shaw,^{1,‡} Alexander V. Sergienko,^{1,2} Bahaa E. A. Saleh,¹ Malvin C. Teich,^{1,2} Aaron J. Miller,³ Sae Woo Nam,³ and John Martinis³

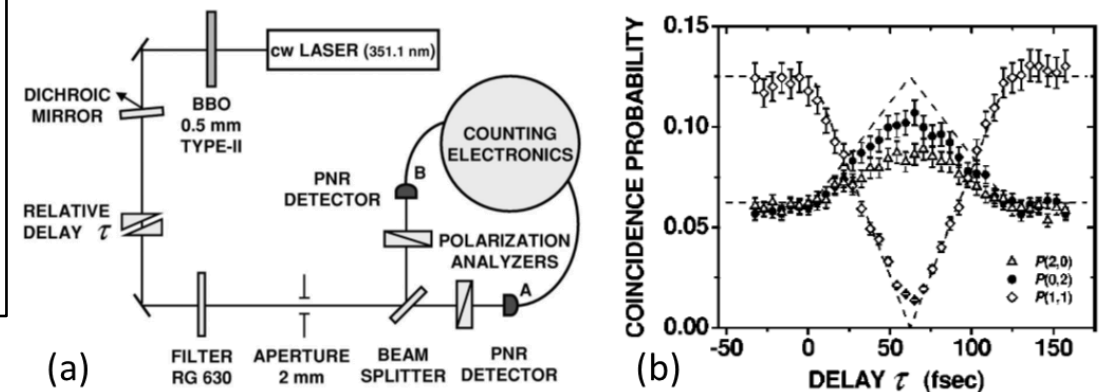
¹Department of Electrical & Computer Engineering, Quantum Imaging Laboratory,[§] Boston University, 8 Saint Mary's Street, Boston, Massachusetts 02215, USA

²Department of Physics, Quantum Imaging Laboratory,[§] Boston University, 8 Saint Mary's Street, Boston, Massachusetts 02215, USA

³National Institute of Standards and Technology, Mail Code 814, 325 Broadway, Boulder, Colorado 80395, USA

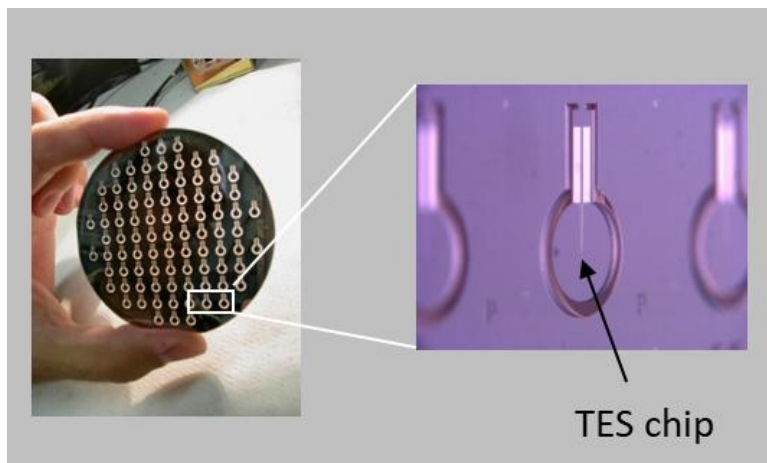
(Received 22 May 2003; published 16 December 2003)

Quantum theory predicts that two indistinguishable photons incident on a beam-splitter interferometer exit together (the pair emerges randomly from one port or the other). We use a special photon-number-resolving energy detector for a direct observation of this quantum-interference phenomenon. Simultaneous measurements from two such detectors, one at each beam-splitter-interferometer output port, confirm the absence of cross coincidences. Photon-number-resolving detectors are expected to find use in other quantum-optics and quantum-information-processing experiments.

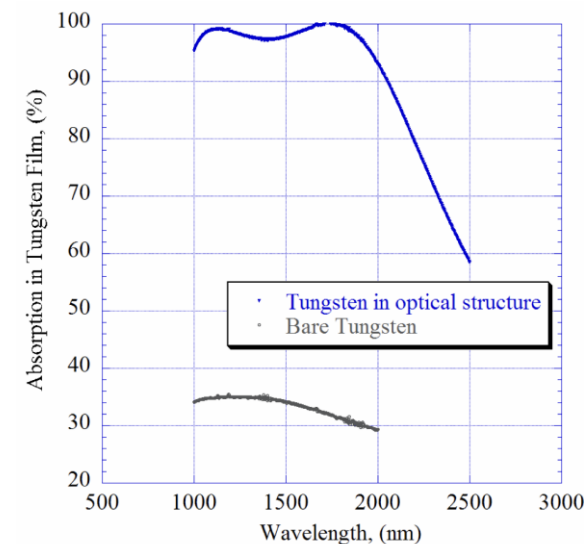
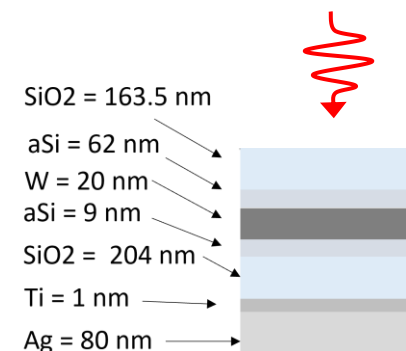
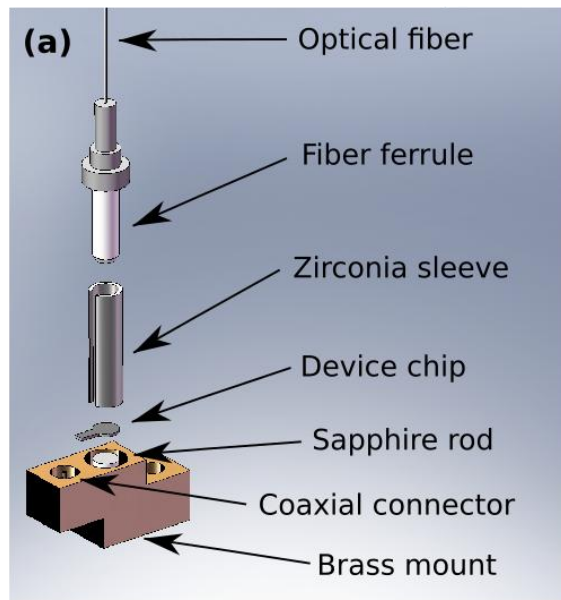


Optical TES System Detection Efficiency (SDE)

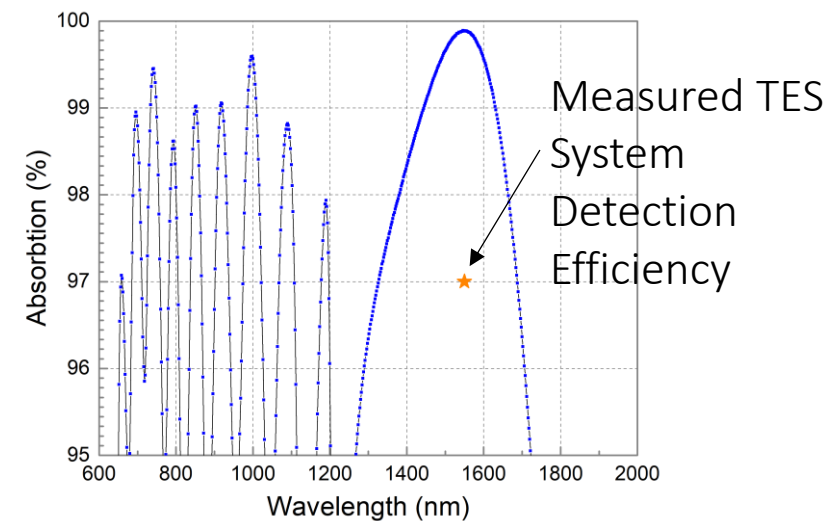
- Coupling Efficiency
- Absorption



Miller et al., *Opt. Express* 19 (10), 9102 (2011)



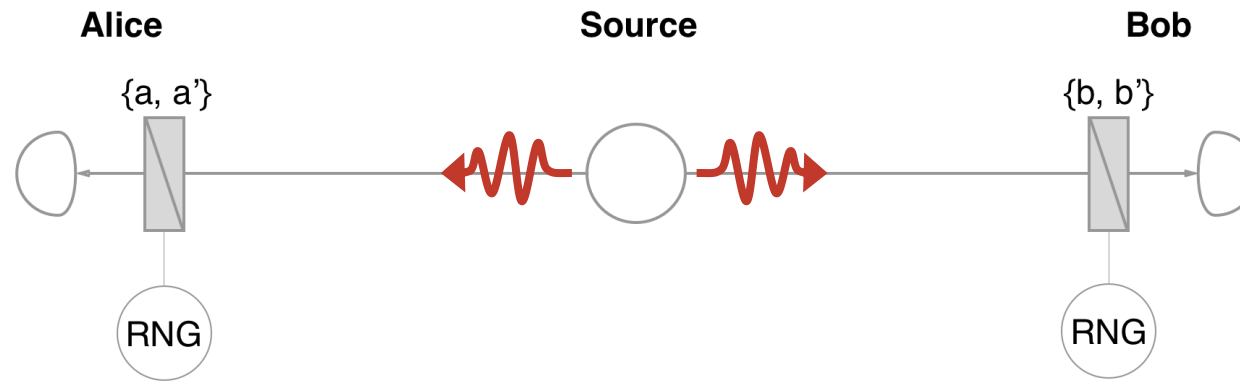
Lita et al, *Opt. Exp.* (2008)



System Detection Efficiency (SDE)	> 98 % @ 1550 nm	Larsen, M.V. et al. <i>Nature</i> 642, (2025).
	≥ 95% @ 1550 nm	Lita, A. E., et al., <i>Opt. Express</i> (2008) Peizhan Li et al., <i>JLTP</i> (2024)
	≥ 98% @ 860 nm	Fukuda, D. et al., <i>Opt. Express</i> (2011)

Loophole-Free Bell Test rules out local realism (2015)

A major step in entanglement verification and distribution was the experimental implementation of loophole-free Bell tests, executed with photonic and matter qubits.



B. Hensen *et al.*, "Loophole-free Bell Inequality Violation Using Electron Spins Separated by 1.3 Kilometres," [Nature 526, 682 \(2015\)](#)

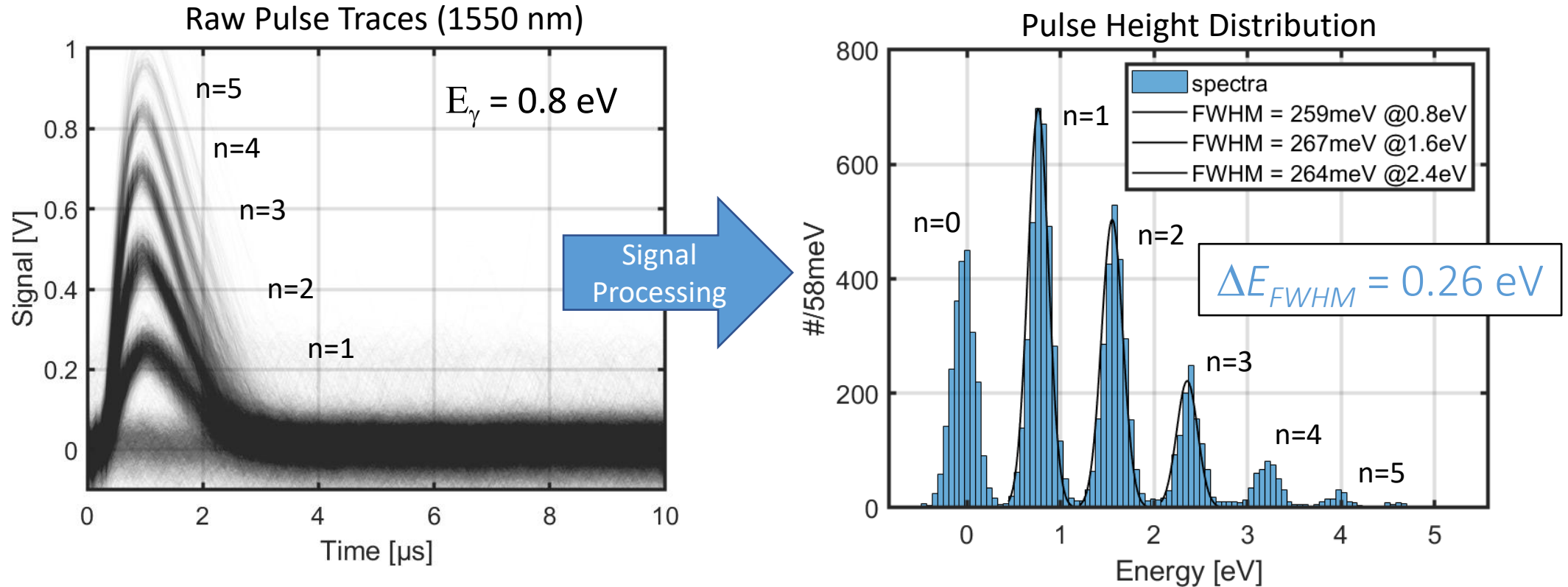
M. Giustina *et al.*, "Significant-Loophole-Free Test of Bell's Theorem with Entangled Photons," [Phys. Rev. Lett. 115, 250401 \(2015\)](#)

L. K. Shalm *et al.*, "Strong Loophole-Free Test of Local Realism," [Phys. Rev. Lett. 115, 250402 \(2015\)](#)

W Optical TES
 $\lambda = 810\text{nm}$
 $\tau \sim 1 \mu\text{s}; \Delta t_{\sigma} \sim 100 \text{ ns}$
SDE > 95%

SNSPD
 $\lambda = 1550\text{nm}$
 $\tau \sim 50 \text{ ns}; \Delta t_{\sigma} \sim 100 \text{ ps}$
SDE > 90%

TES Photon-Number Resolution



Use optimum matched filter post-processing for improved signal-to-noise ratio

TES Photon-Number Resolution

How high a photon number is distinguishable with a TES?

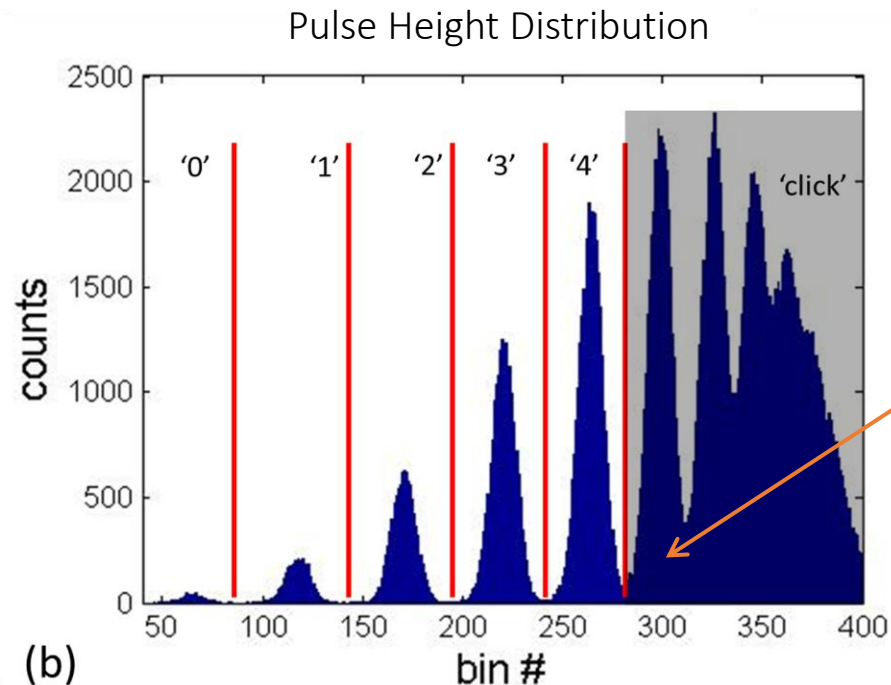
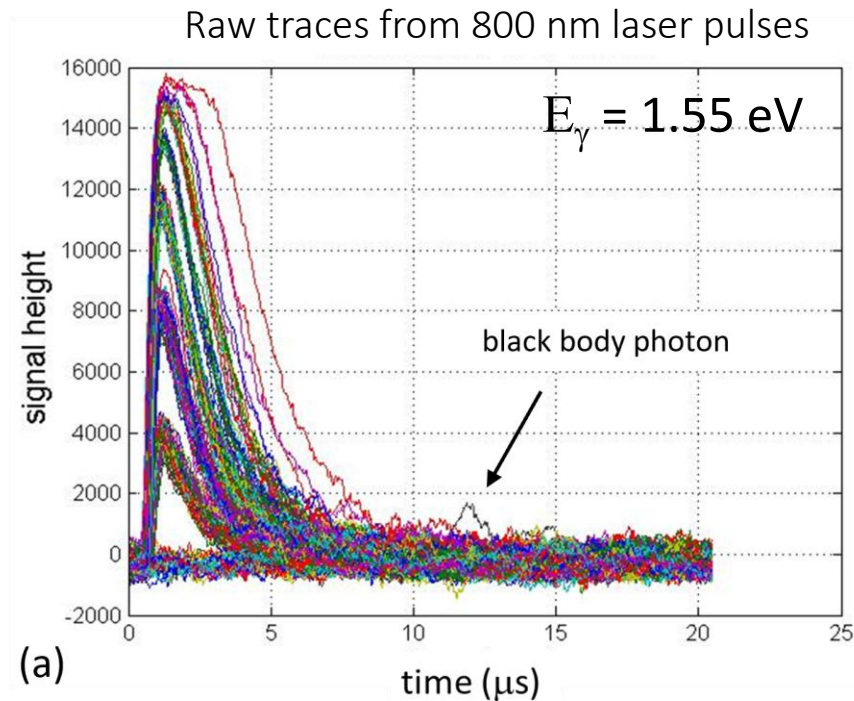
- Photon energy E_γ and ΔE_{FWHM}
- Device design/Saturation energy

$$\Delta E_{FWHM} \approx 2\sqrt{2\ln 2} \sqrt{4k_B T_c^2 \frac{C}{\alpha} \sqrt{n/2}}$$

$$E_{sat} \approx T_c C / \alpha$$

How accurately can we distinguish photon numbers?

- Photon number peaks separation (Error < 1% -> peaks separation > 6 σ)



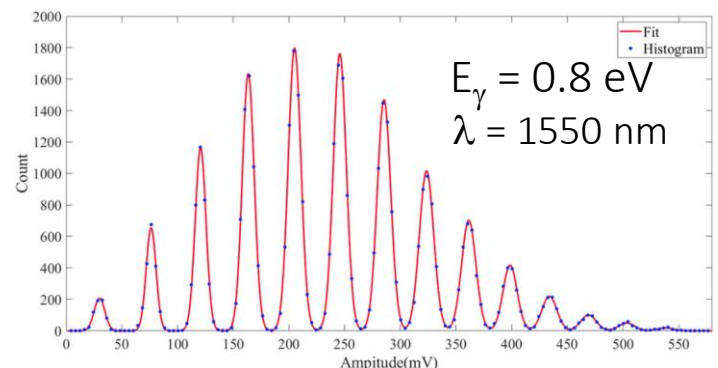
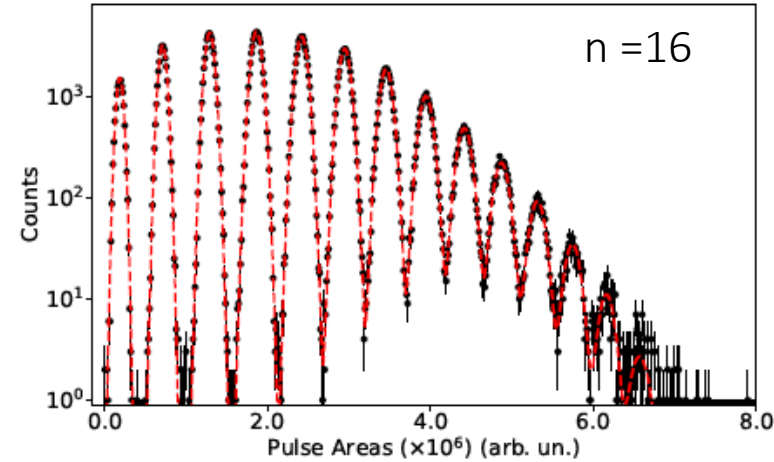
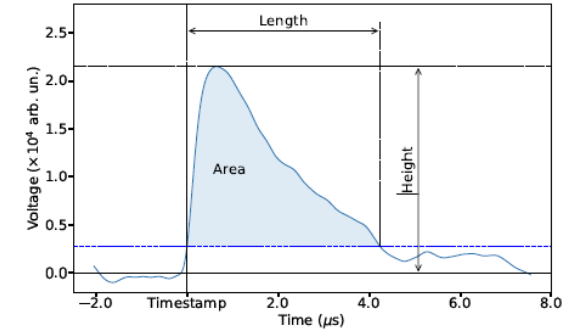
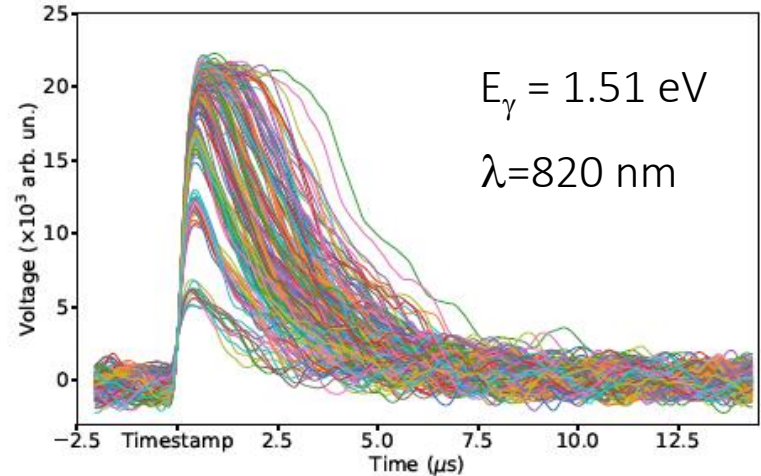
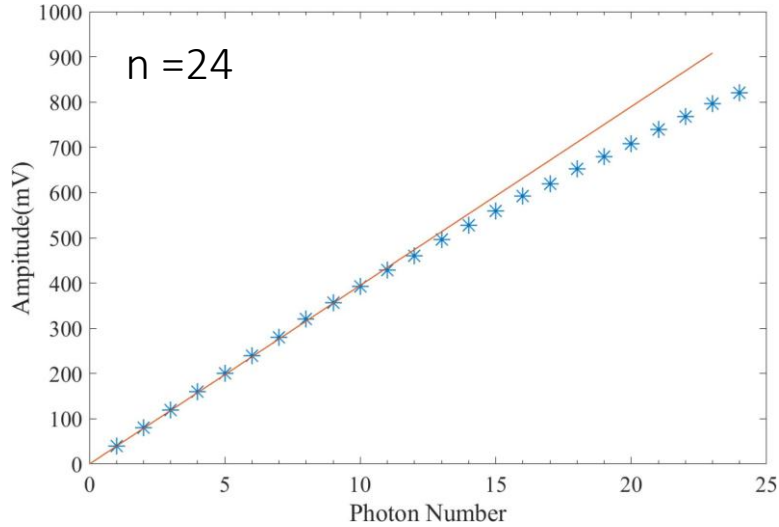
Above a certain photon energy, TES is no longer operating in a linear regime

T. Gerrits et al., Superconducting Devices in Quantum Optics (2016)

Light-based Quantum Technologies, April 16, 2026

TES Photon-Number Resolution

Extend PNR beyond linear operation regime



Hong-Fan Zhang et al., IEEE Transactions on Applied Superconductivity, 34, (2024)

Probabilities of correct Photon number assignment

$$n < 10, \quad p > 99\%$$

$$10 > n < 16, \quad p > 90\%$$

$$\Delta E_{FWHM} \leq 0.59 \text{ eV (1.51 eV)}$$

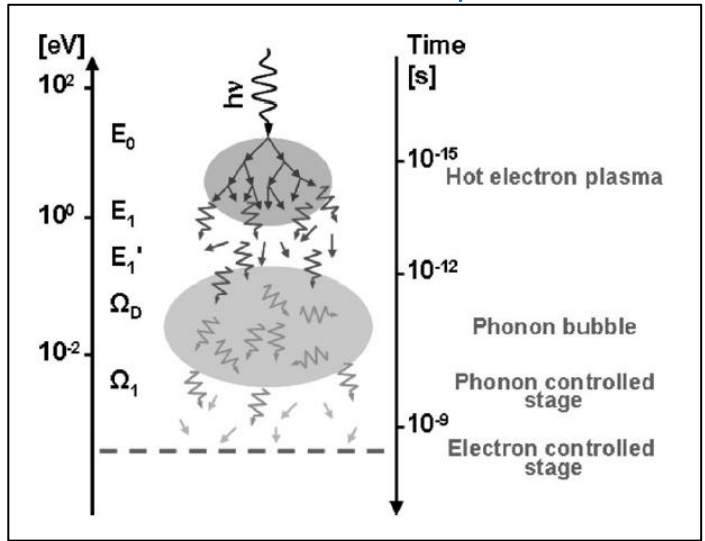
$$\Delta E_{FWHM} \leq 0.31 \text{ eV (0.8 eV)}$$

L.A. Morais et al., Quantum 8, 1355 (2024)

Optical TES Energy Resolution Optimization

- Downconversion phonon noise and energy collection efficiency

Schematic photon energy downconversion in a superconductor

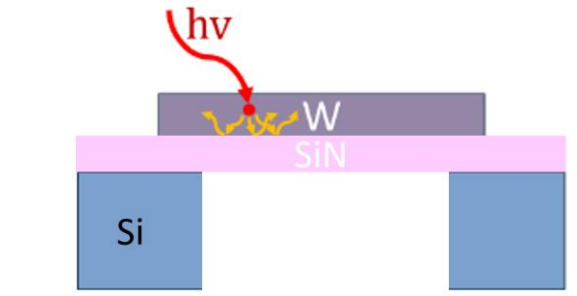


A.G. Kozorezov, et. al., *Physical Review B* 75 (2007)

$$\Delta E_{\text{Irwin/Hilton \& Kozorezov}} \approx 2.355 \sqrt{\frac{4k_B T_c E_{max}}{1 + \beta} \sqrt{\frac{nF(T_c, T_b)}{1 - (T_b/T_c)^n} \frac{\sqrt{\xi}}{\kappa^2}} + J(E)E}$$

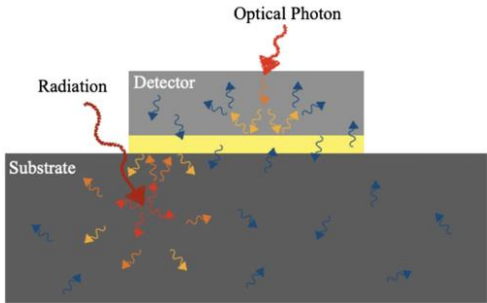
Energy collection efficiency: κ
 Downconversion Phonon Noise: $J(E)$

- Fabrication on membranes allow escaped phonons to be recaptured in the sensor before reaching the substrate



Lita, A.E. et al., *JLTP* 151, 125 (2008)

- Acoustically mismatched substrates block high energy phonons to escape detector material.

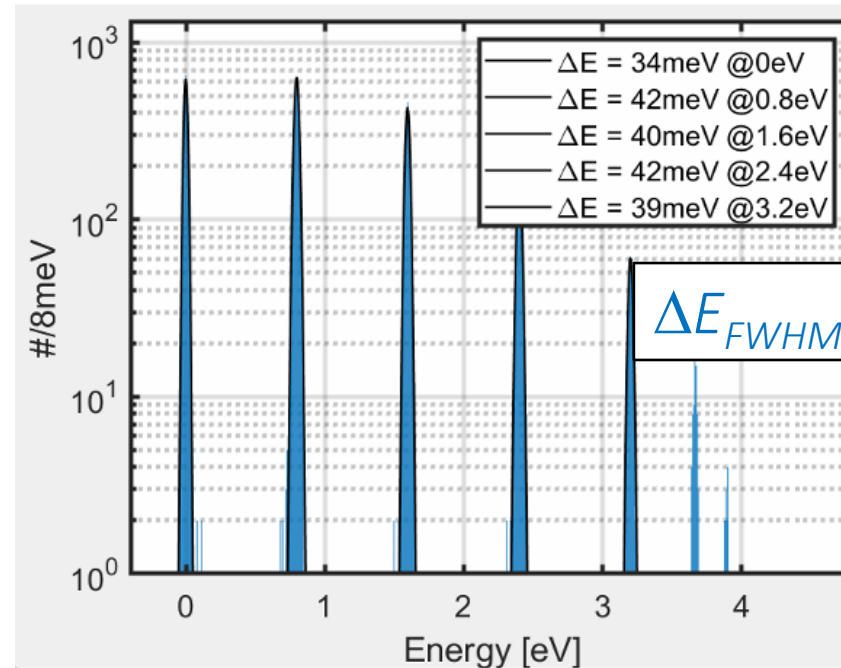
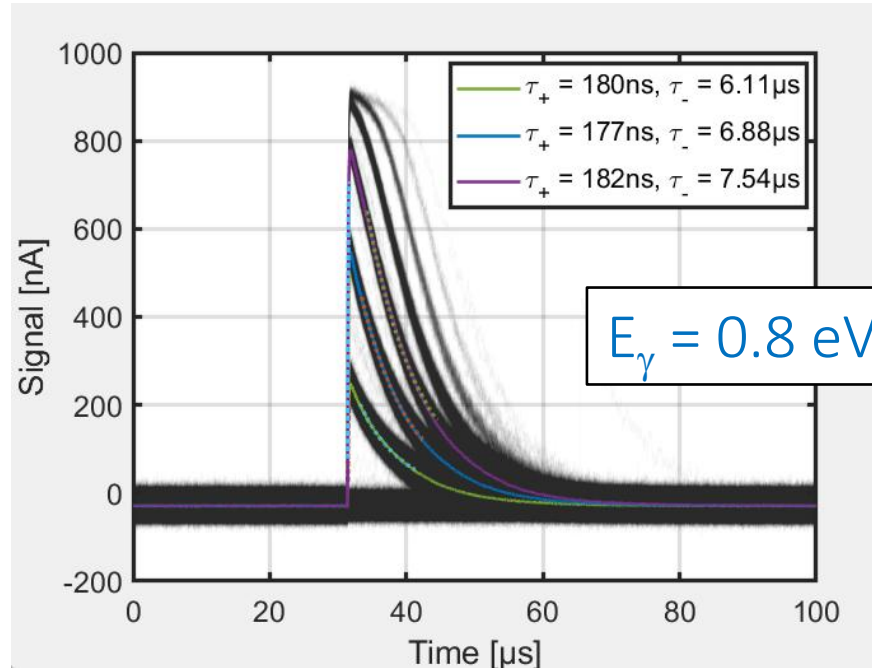
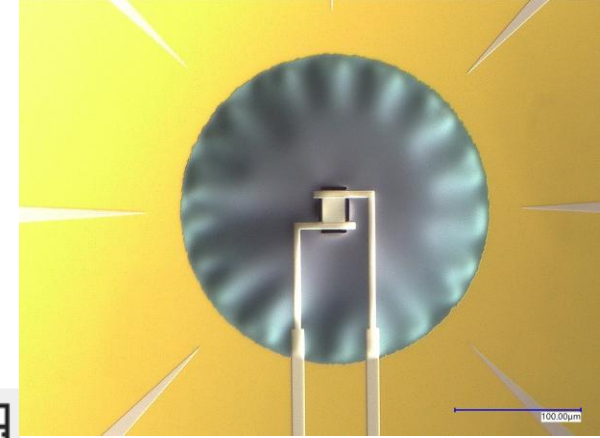


Zobrist N., et al. *PRL* 129(1):017701 (2022)

Optical TES device optimization

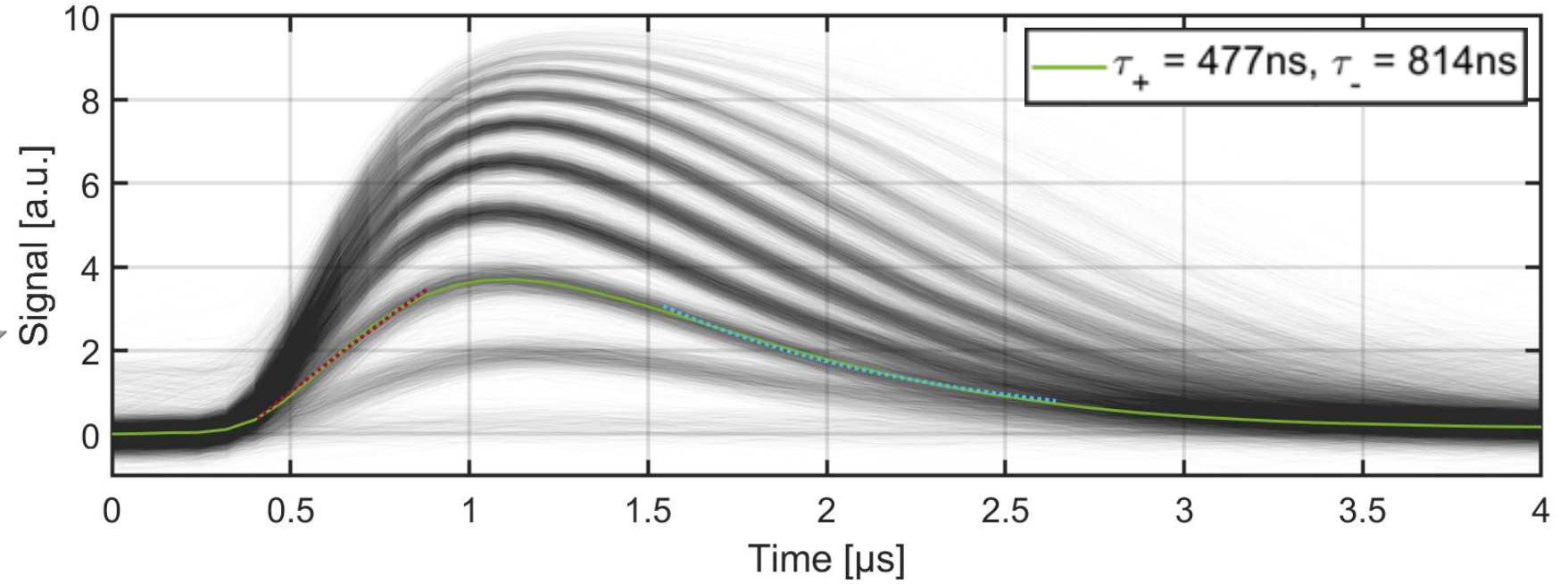
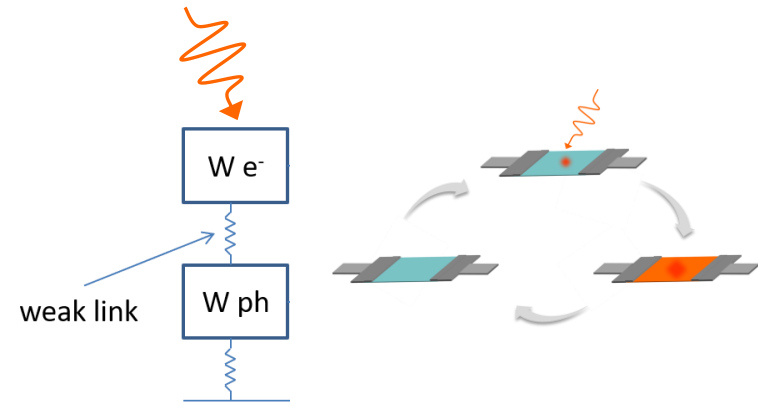
- Energy Resolution and Speed tradeoff

$$R = E/\Delta E = 20 \quad 1550 \text{ nm}$$



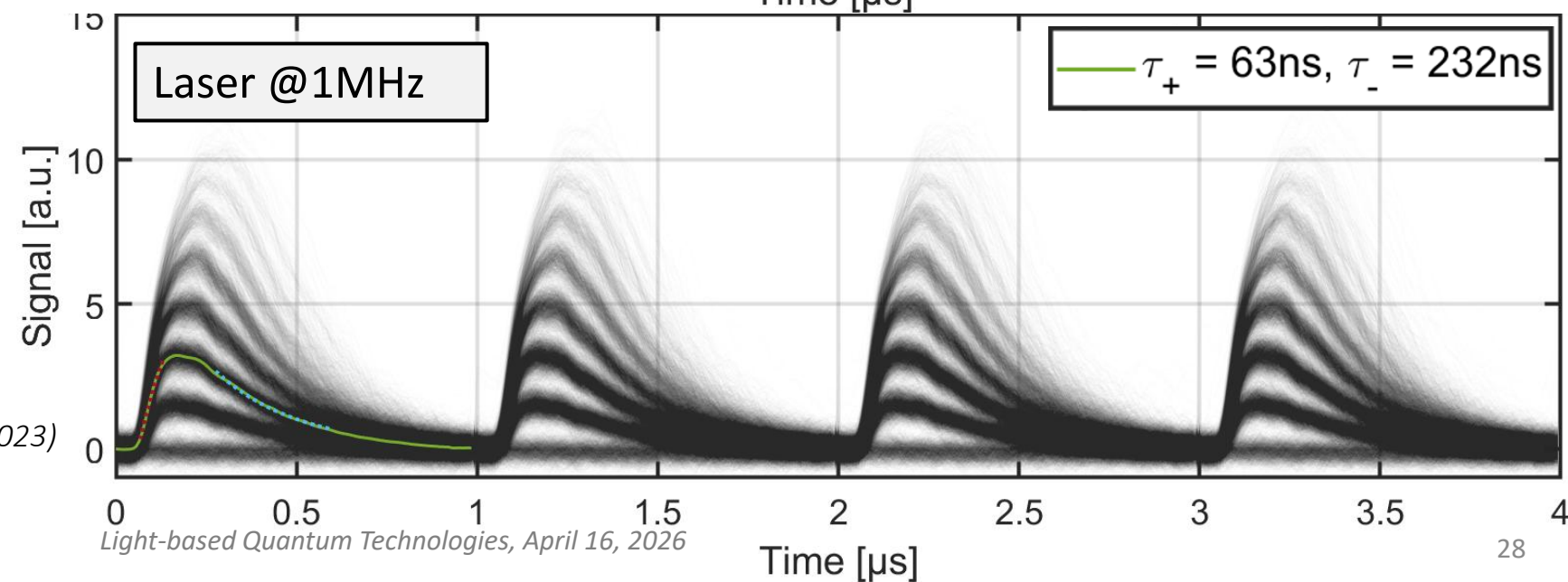
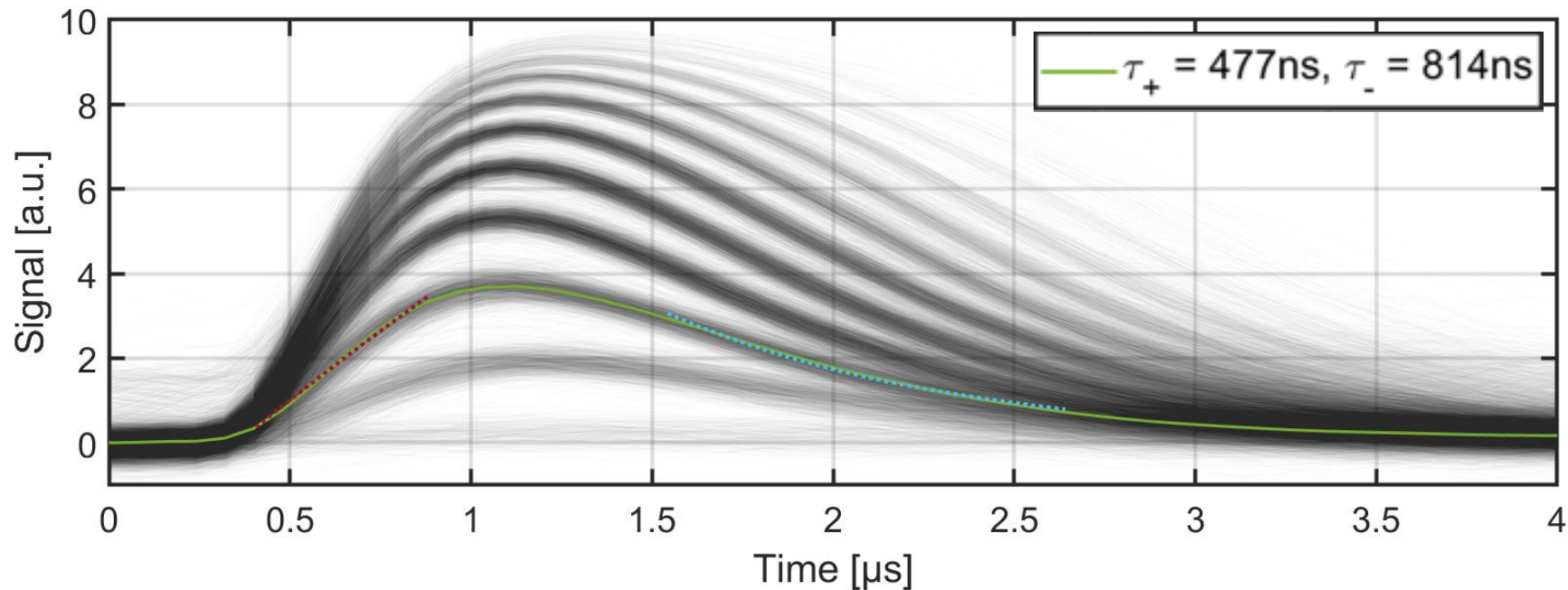
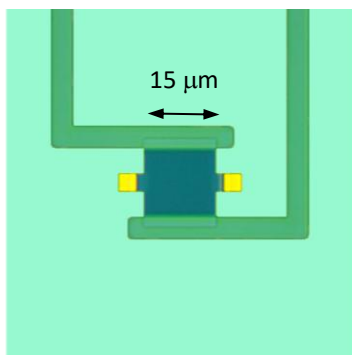
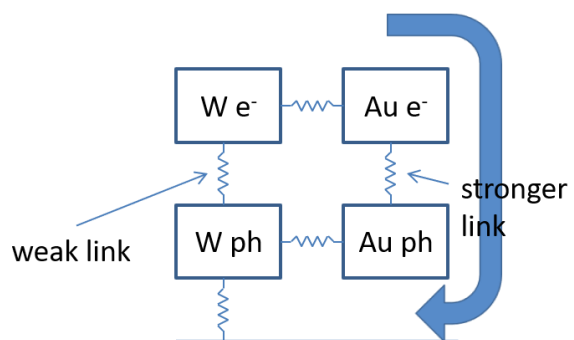
- Record Energy resolution at 1550 nm
- Longer device recovery time

Optical TES Recovery Time



Optical TES Recovery Time

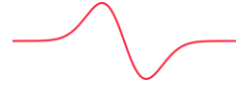
Thermal link engineering
High bandwidth readout



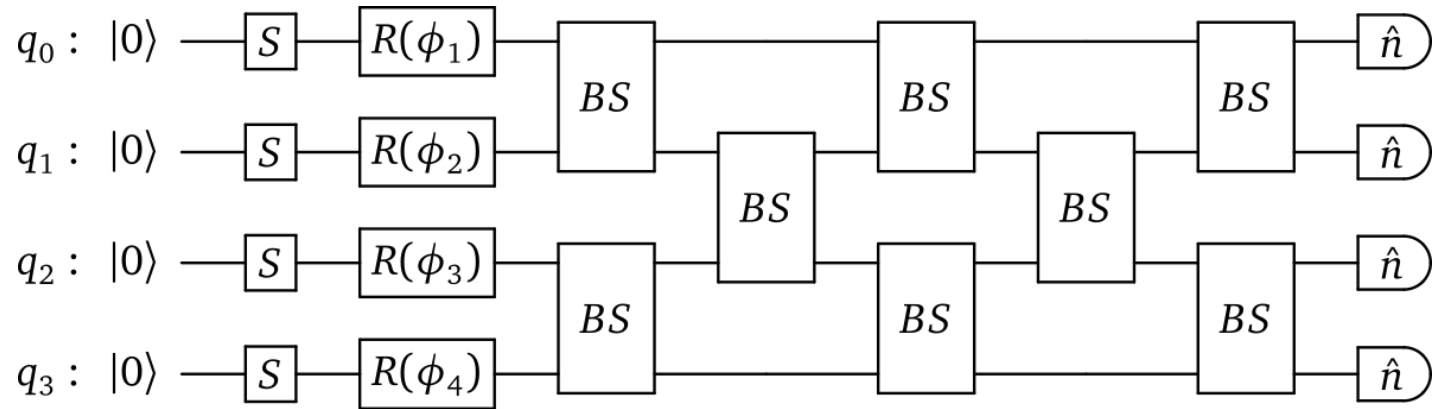
Hummatov R. et al, *J. Appl. Phys.* 133, 234502 (2023)

Photonic Quantum Computing

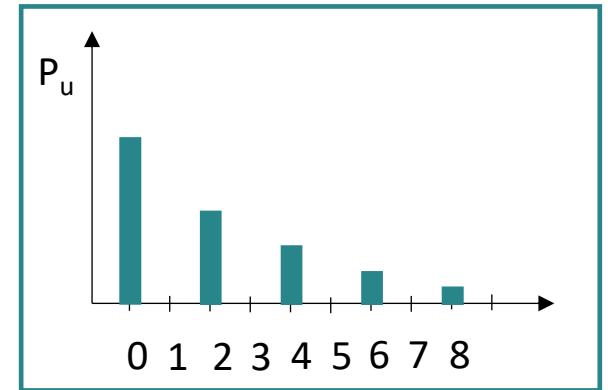
Continuous Variable (CV) States



Gaussian Boson Sampling (GBS) – generates qubit states (CV)



$$\begin{aligned} |\psi\rangle &= c_0|0\rangle + c_1|1\rangle \\ &+ \dots + c_n|n\rangle + \\ &= \sum_{n=0}^{\infty} c_n|n\rangle \end{aligned}$$



Courtesy of Xanadu

n photon sources

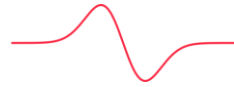
linear interferometer composed of
beam splitters and phase shifters

PNR detectors

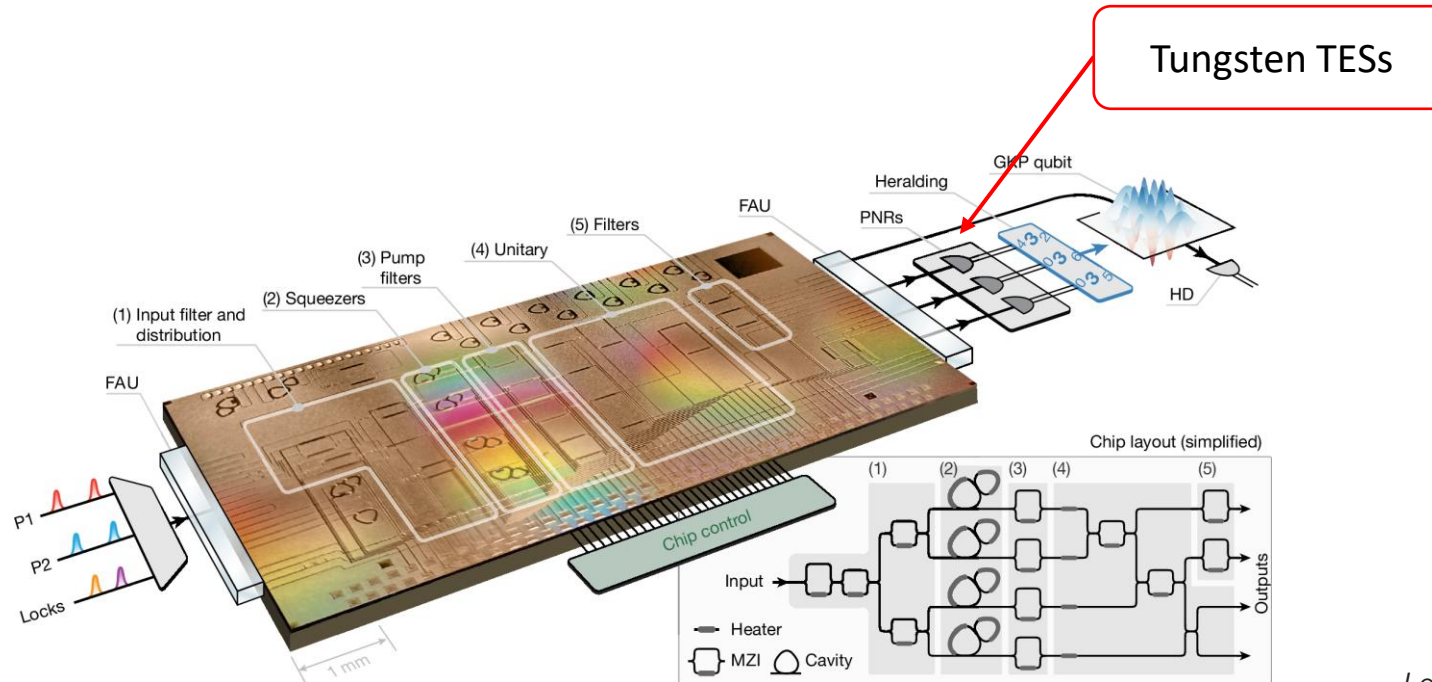
- Information encoded in a continuous variable such as the amplitude and phase of a non-classical light state: squeezed light
- PNR detectors are heralding qubit states at the remaining output modes of the GBS device

Photonic Quantum Computing

Continuous Variable (CV) States



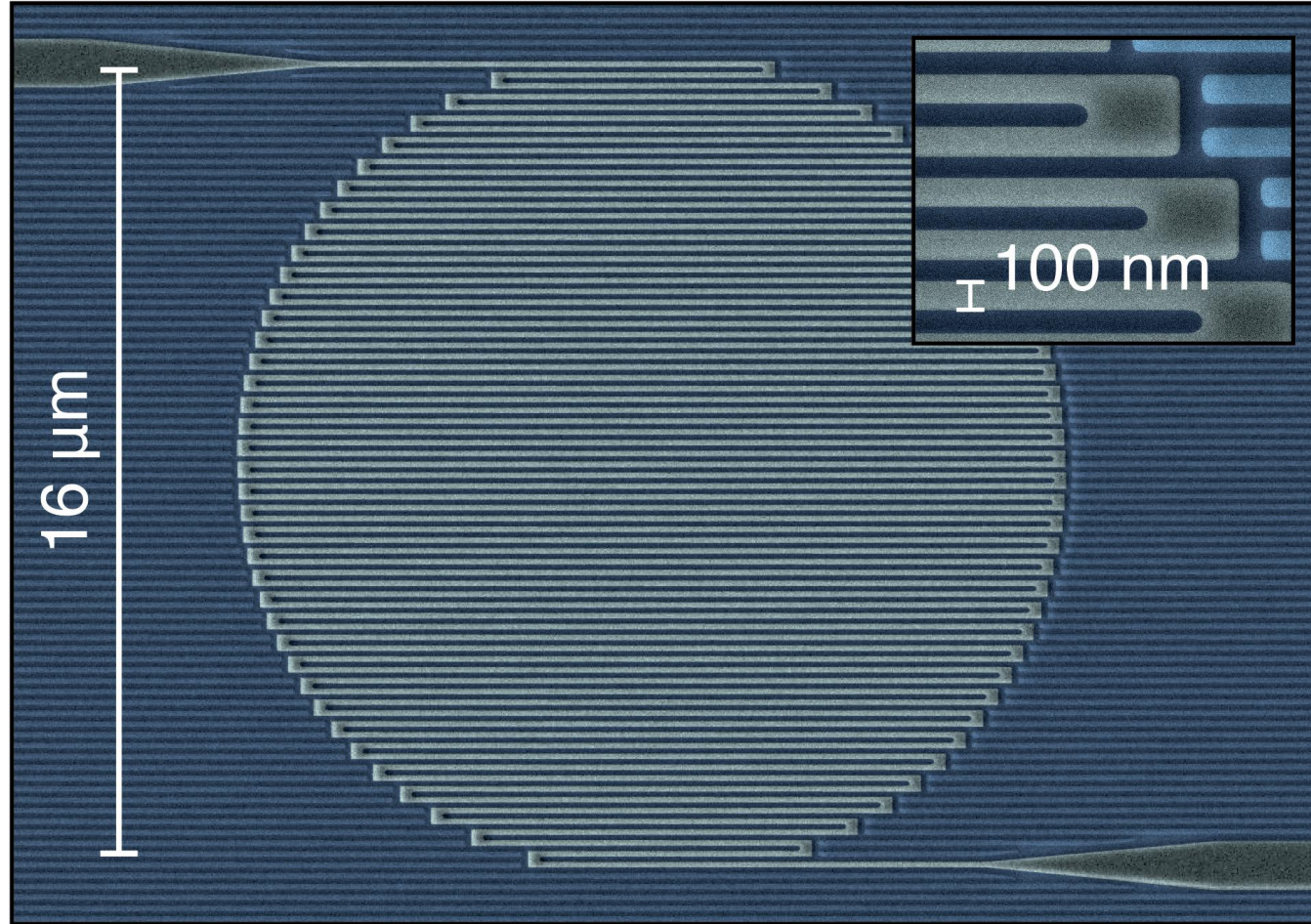
- Tungsten TES detectors are employed as the PNR detectors due to their near-unity detection efficiency, intrinsic photon-number resolution and very low dark count rates.



Larsen, M.V. et al. Nature (2025)

- Photonic quantum advantage machine with all gates programmable
- Demonstrate scalable generation of GKP states
- TES @ 200 kHz; DE: 96%, 98%, 99% PNR = 7 ; $p_m^n > 99\%$

Superconducting Nanowire Single-Photon Detectors (SNSPD)



Superconducting Nanowire Single-Photon Detectors (SNSPD)

APPLIED PHYSICS LETTERS

VOLUME 79, NUMBER 6

6 AUGUST 2001

Picosecond superconducting single-photon optical detector

G. N. Gol'tsman,^{a)} O. Okunev, G. Chulkova, A. Lipatov, A. Semenov, K. Smirnov, B. Voronov, and A. Dzardanov

Department of Physics, Moscow State Pedagogical University, Moscow 119435, Russia

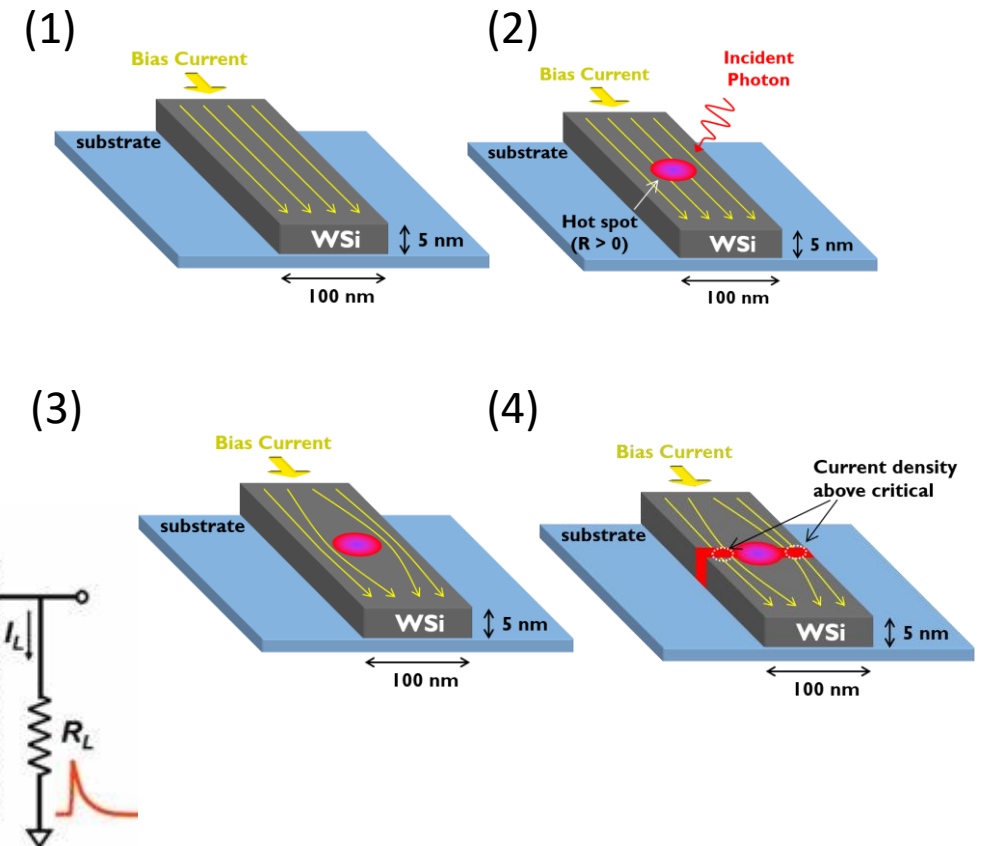
C. Williams and Roman Sobolewski^{b)}

Department of Electrical and Computer Engineering and Laboratory for Laser Energetics, University of Rochester, Rochester, New York 14627-0231

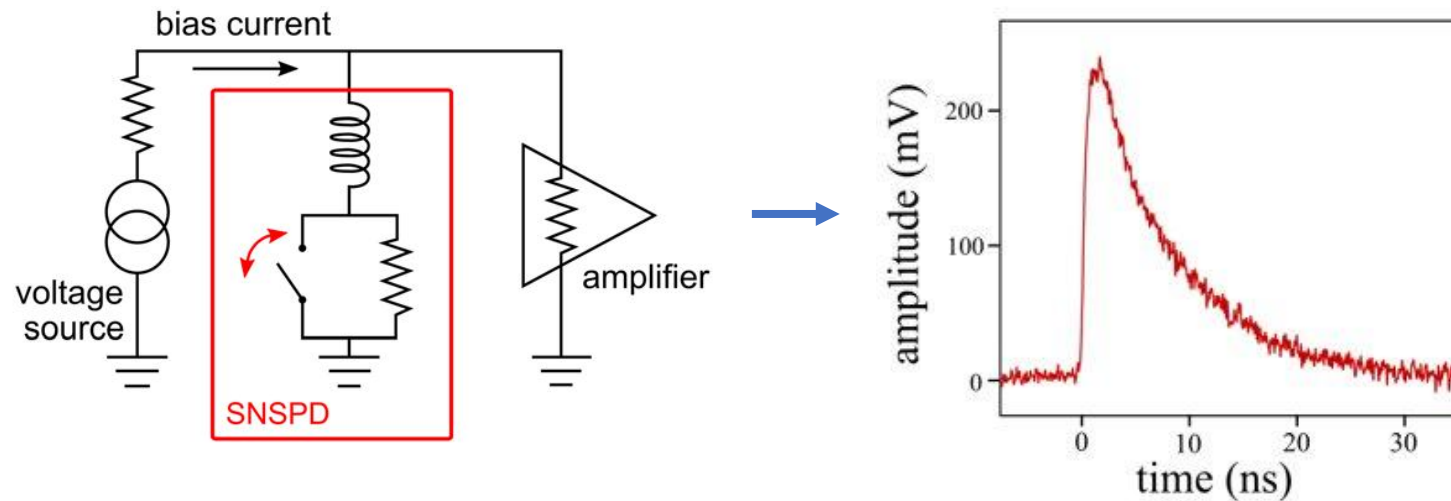
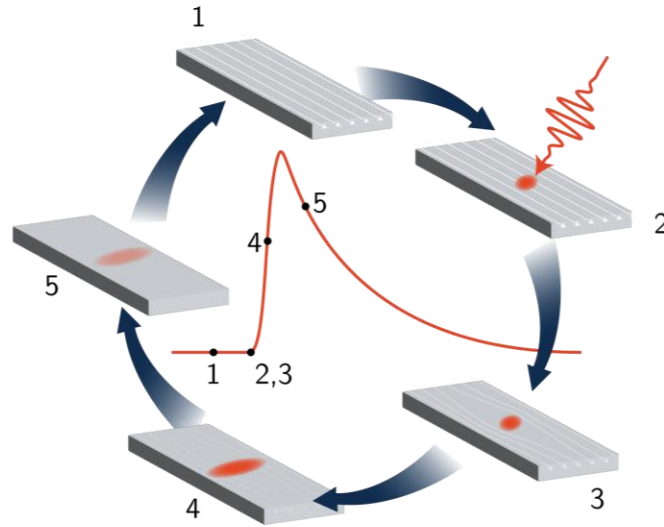
(Received 22 January 2001; accepted for publication 1 June 2001)

We experimentally demonstrate a supercurrent-assisted, hotspot-formation mechanism for ultrafast detection and counting of visible and infrared photons. A photon-induced hotspot leads to a temporary formation of a resistive barrier across the superconducting sensor strip and results in an easily measurable voltage pulse. Subsequent hotspot healing in ~ 30 ps time frame, restores the superconductivity (zero-voltage state), and the detector is ready to register another photon. Our device consists of an ultrathin, very narrow NbN strip, maintained at 4.2 K and current-biased close to the critical current. It exhibits an experimentally measured quantum efficiency of $\sim 20\%$ for $0.81 \mu\text{m}$ wavelength photons and negligible dark counts. © 2001 American Institute of Physics

[DOI: 10.1063/1.1388868]

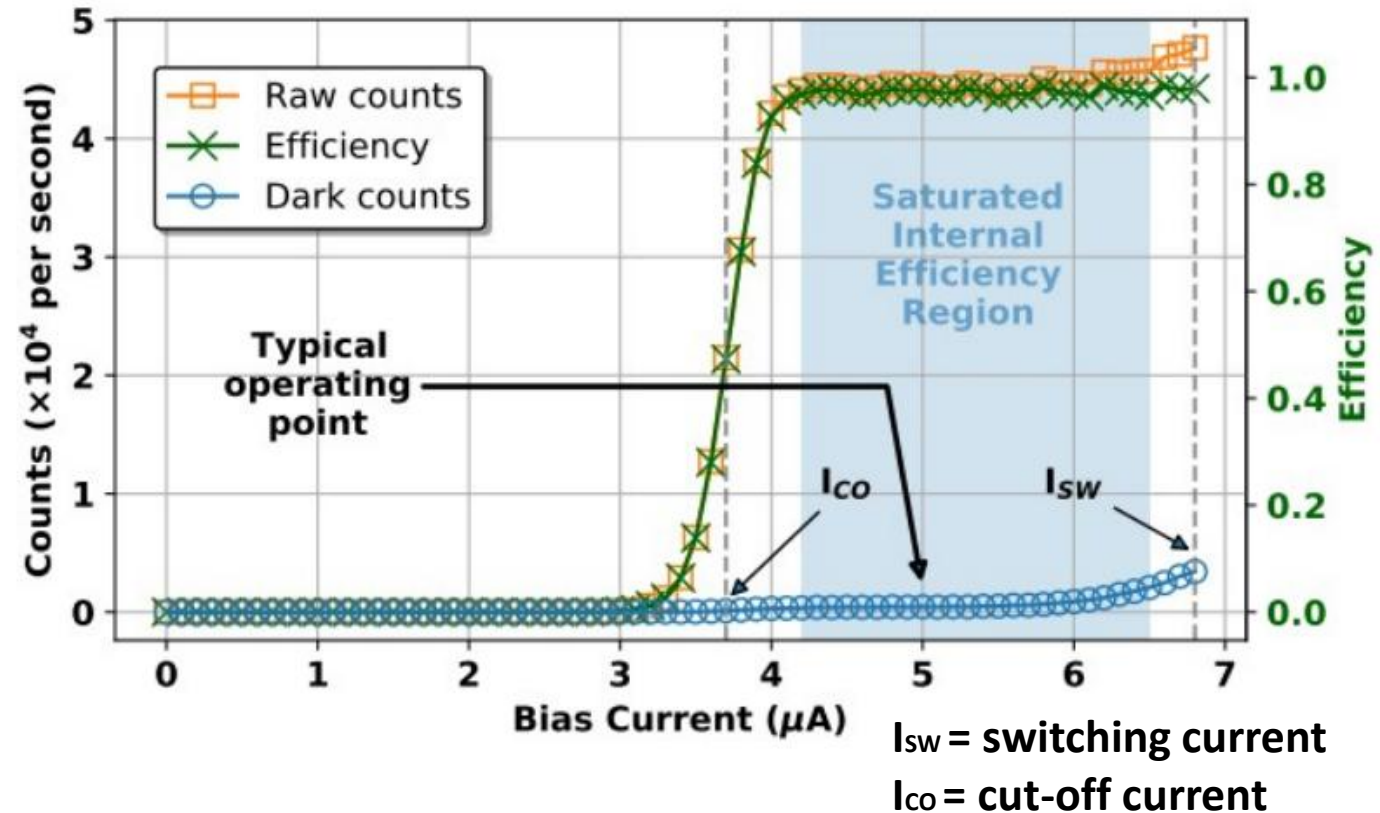
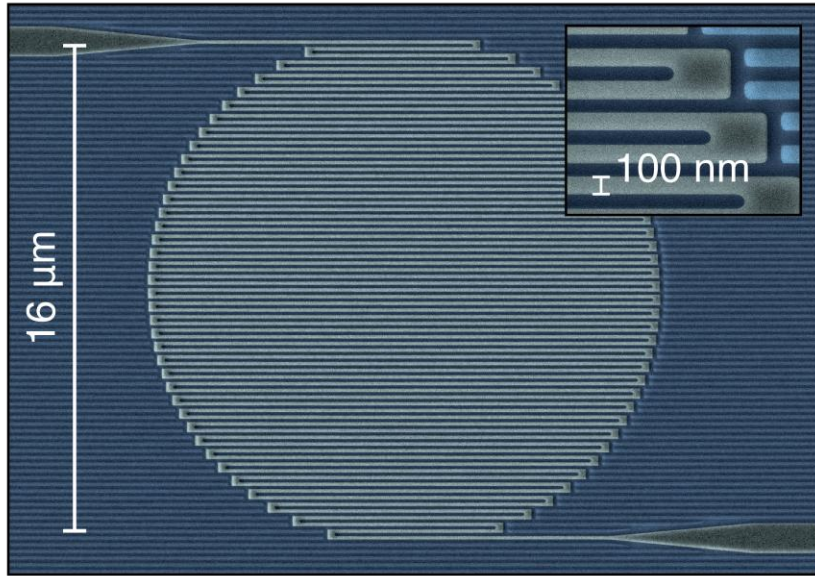


Superconducting Nanowire Single Photon Detectors (SNSPD)



- Superconducting wire current biased close to critical current, I_c
- Very fast, like a switch
- Rise time < 100 ps
- Pulse duration \sim 1-100ns
- Truly digital detection mechanism – reduced drift and zero read noise
- No energy resolution
- Operating temperature 1-4 K in most cases

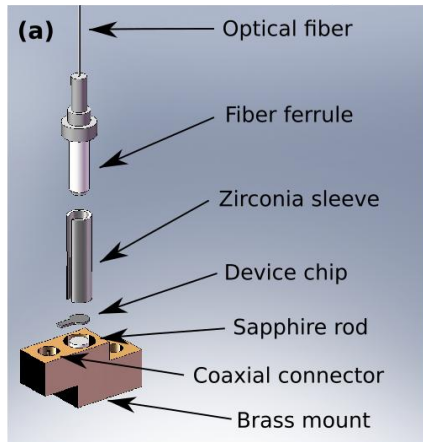
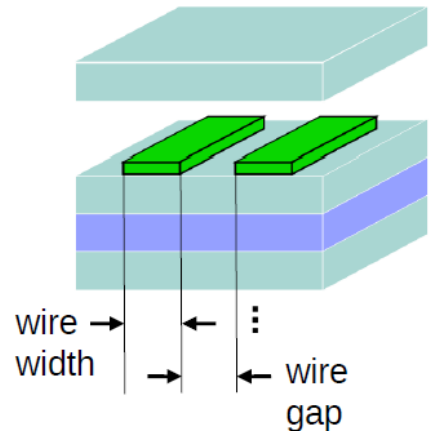
Basic SNSPD Characterization



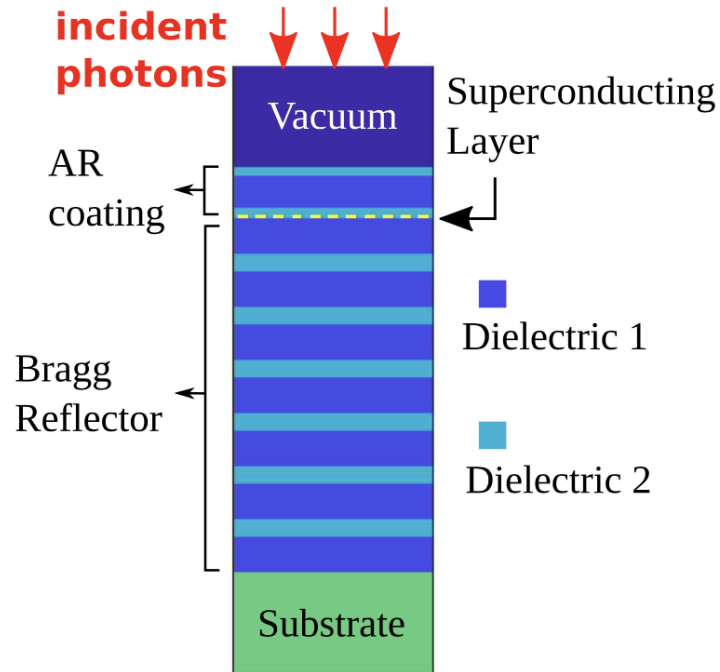
SNSPD materials:

- WSi 3.5 K, MoSi 6 K (amorphous)
- NbN ~ 10 K, NbTiN ~ 10 K (polycrystalline)
- MgB_2 ~ 20 K (polycrystalline); Charaev, I, et al. Nat Commun 15, 3973 (2024)

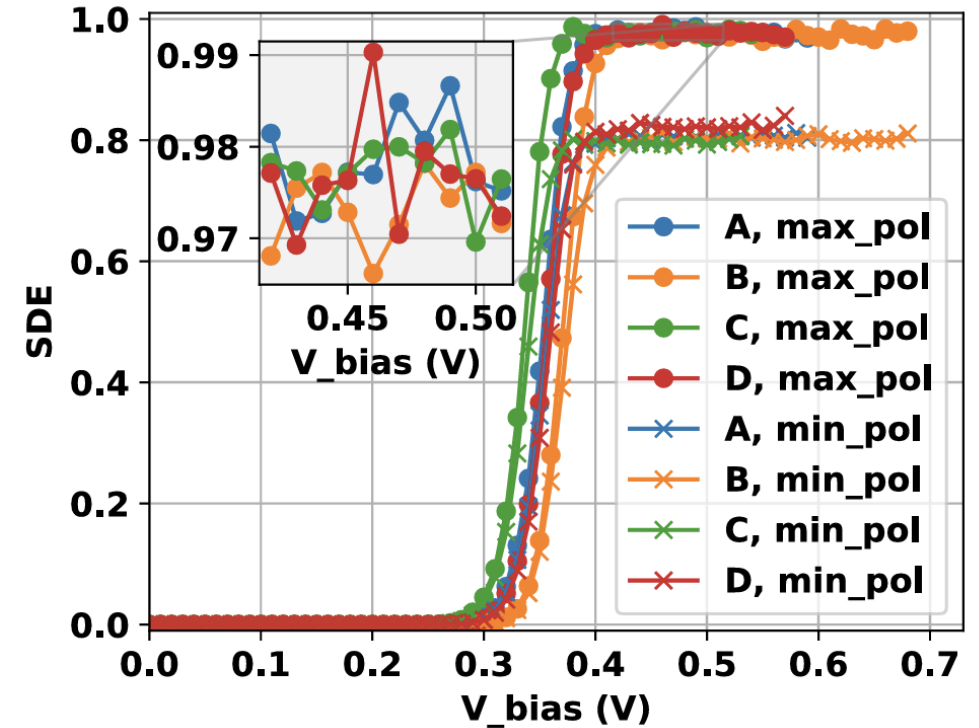
System Detection Efficiency (SDE)



Miller et al., Opt. Express (2011)



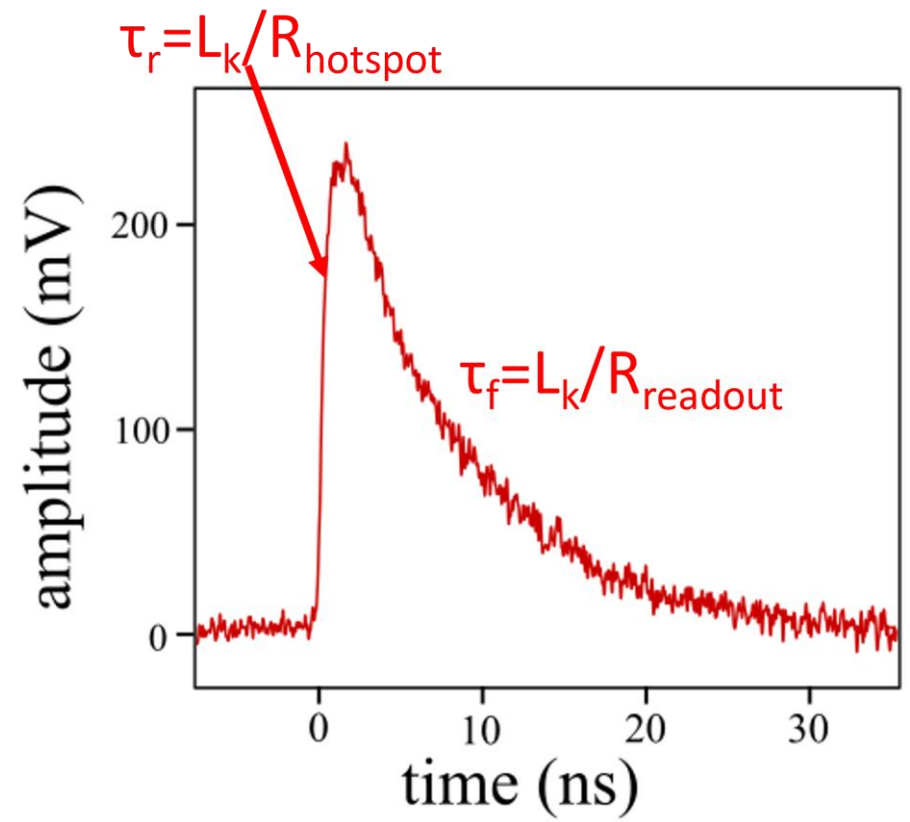
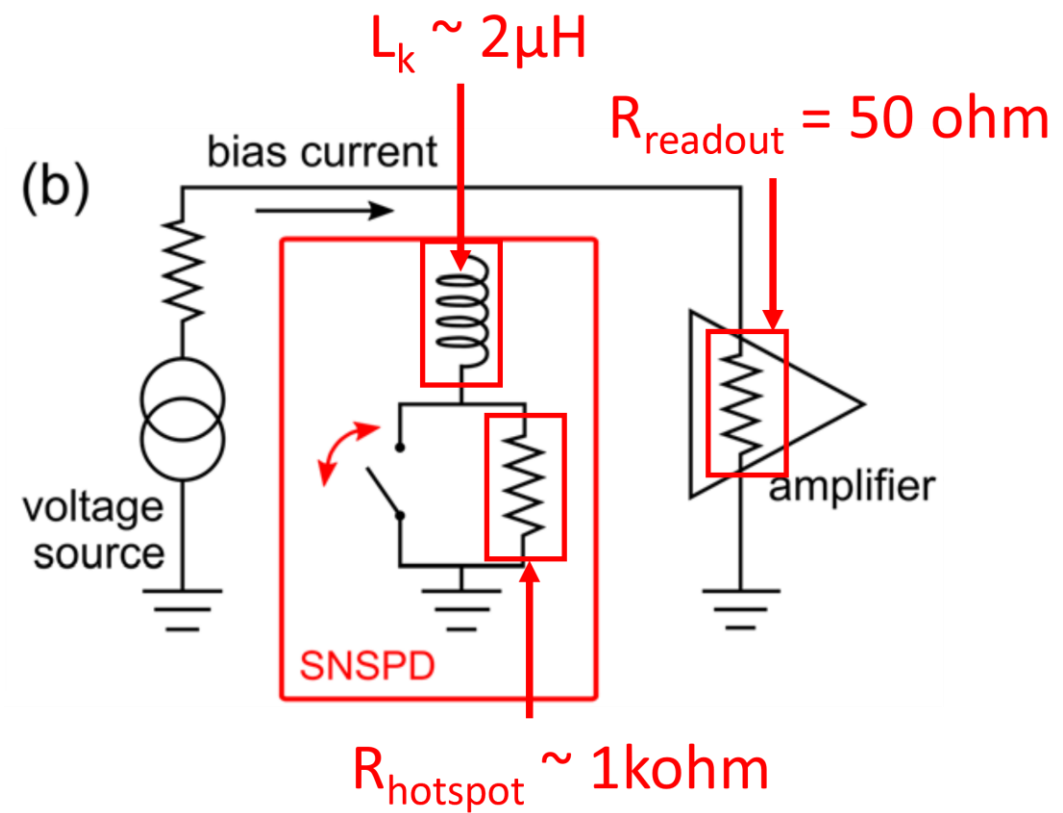
System detection efficiency at 1550 nm



D. Reddy, *Optica* 7, 1649 (2020)

System Detection Efficiency (SDE) @ 1550 nm	$\geq 98\%$	D. V. Reddy et al., <i>Optica</i> (2020) P. Hu et al., <i>Opt. Express</i> (2020) J. Chang et al., <i>APL Photonics</i> (2021)
---	-------------	--

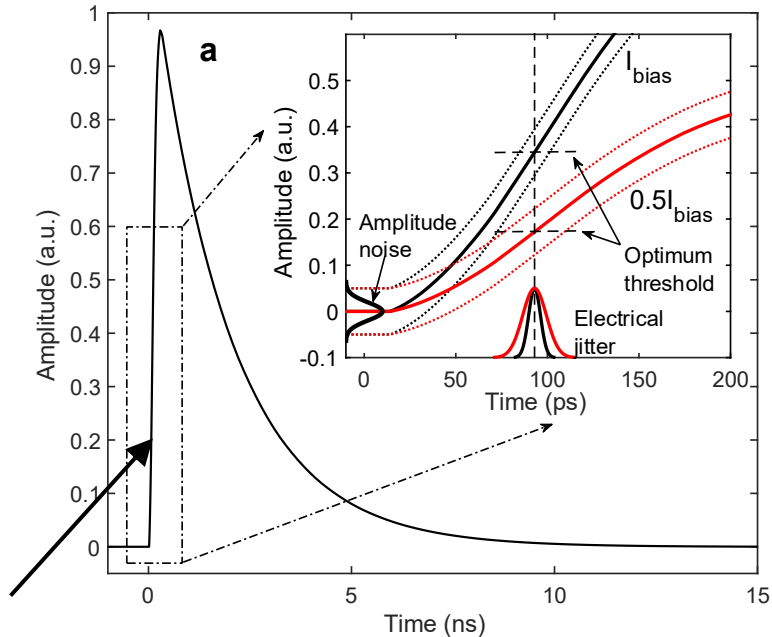
SNSPD Rise Time and Recovery Time



L_k is proportional to the length of the nanowire
Larger detectors will have longer “dead time”

SNSPD Timing Jitter: The Rising Edge

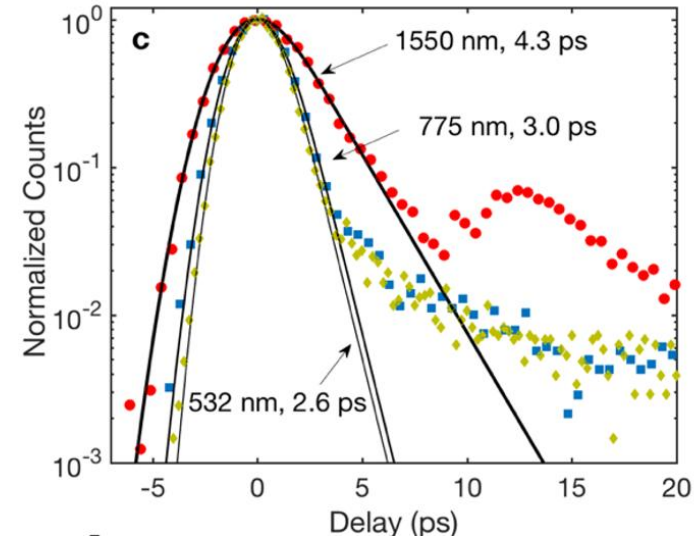
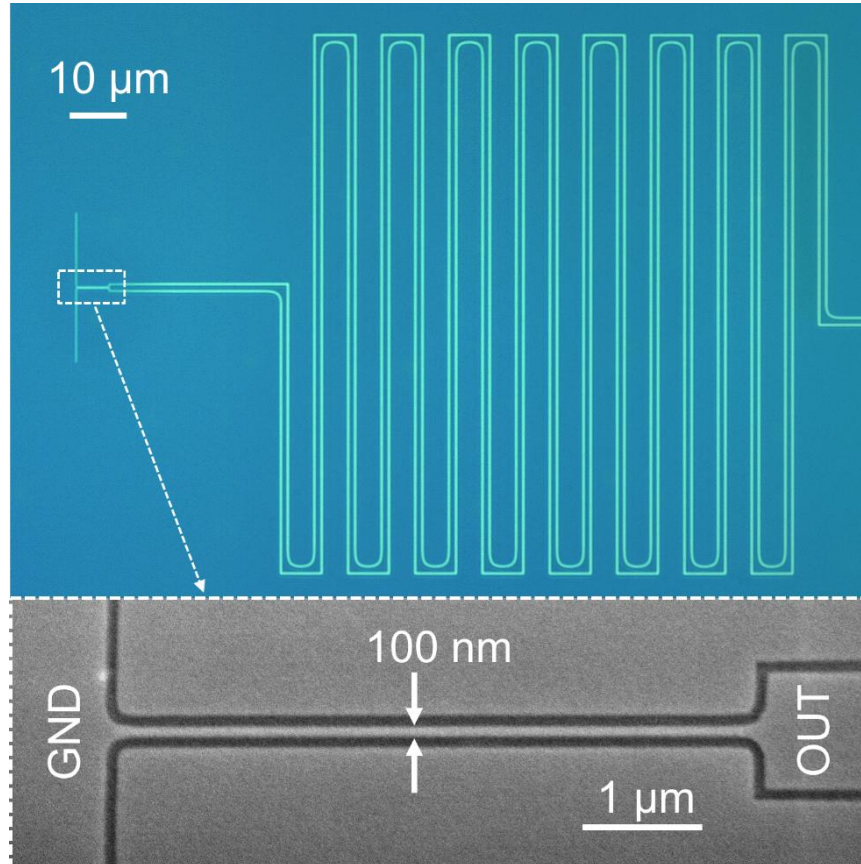
Timing record: ~ 4 ps jitter at 1550 nm



"Slew Rate"
(V/ns)

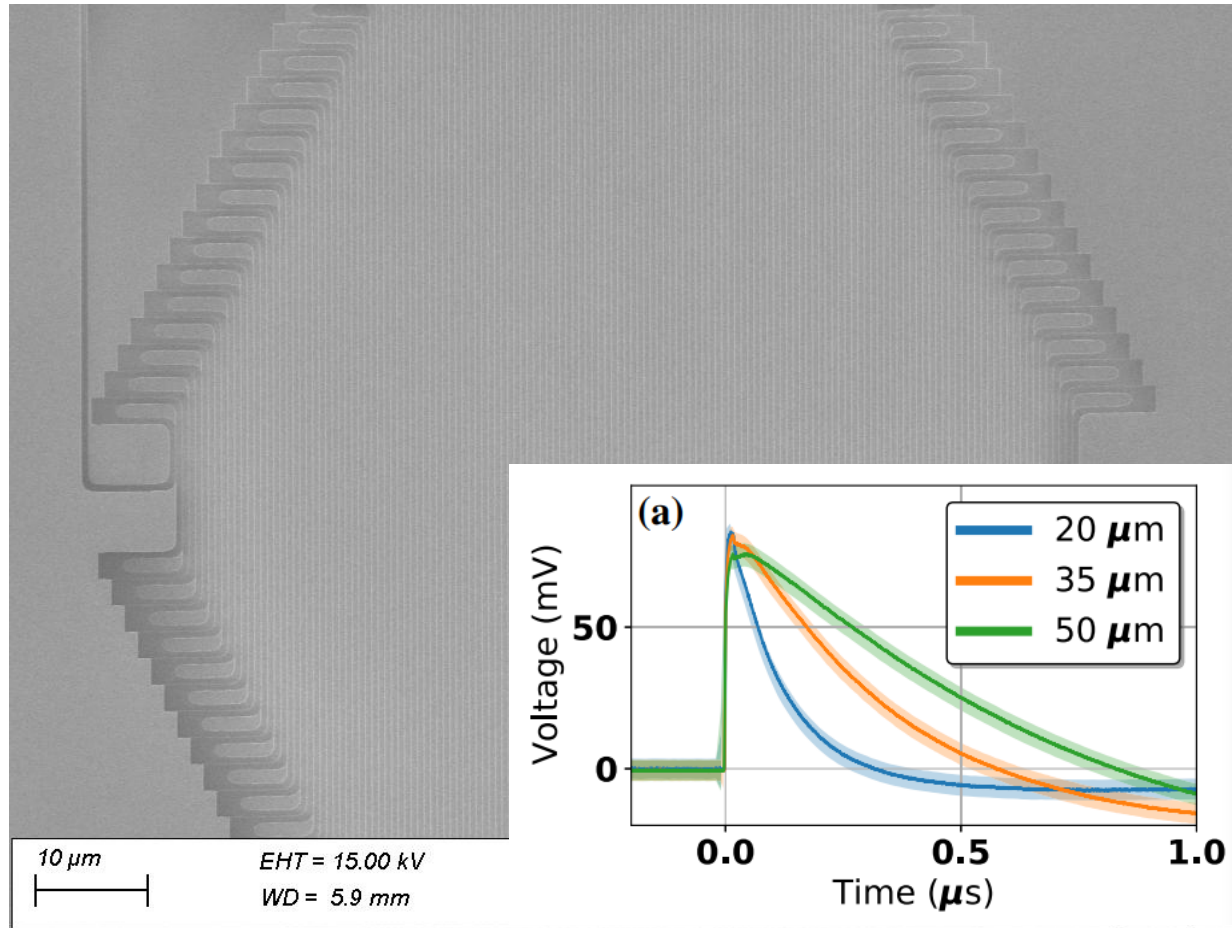
$$\sigma_T = \frac{\sigma_V}{\text{Slope}}$$

Slower Slew Rate -> Degraded Jitter
 Large Inductance -> Slower Slew Rate
 $(\tau_r = L_k / R_{hotspot})$
 Large Area Detector -> Large Inductance

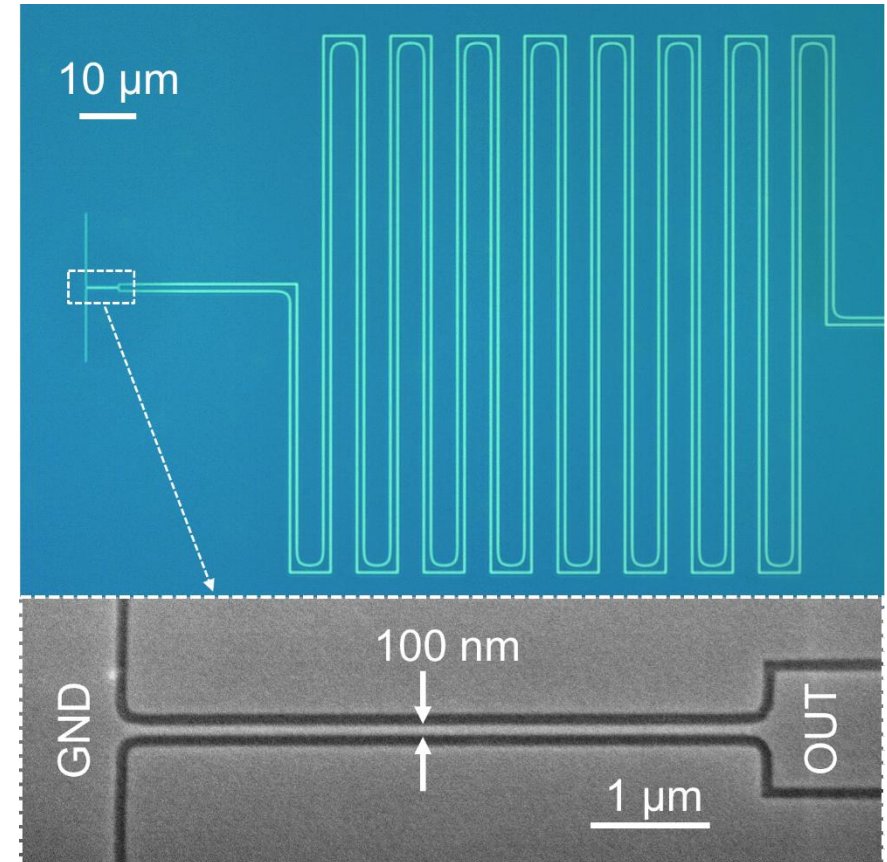


B. Korzh, *Nature Photonics* **14**, 250 (2020)

Speed/Detection Efficiency Tradeoff



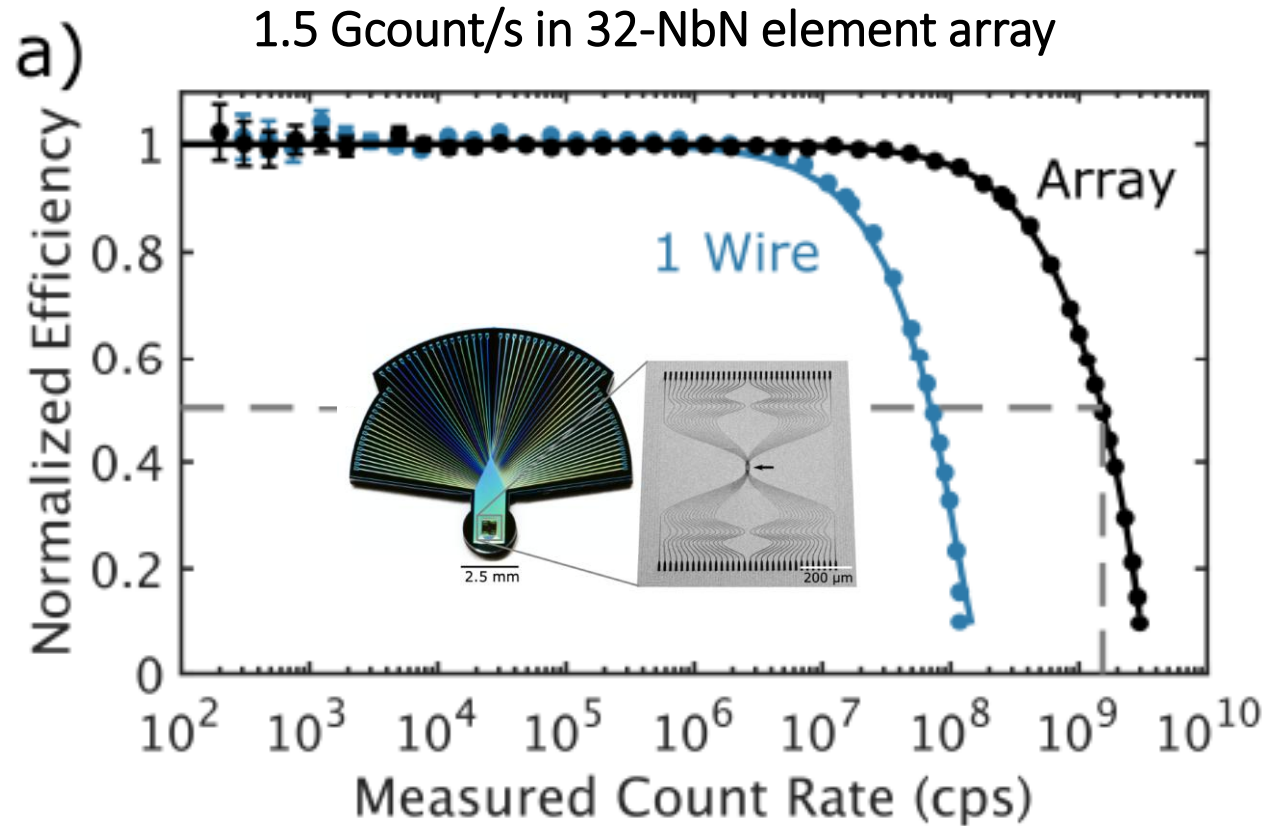
D. Reddy, *Optica* **7**, 1649 (2020)



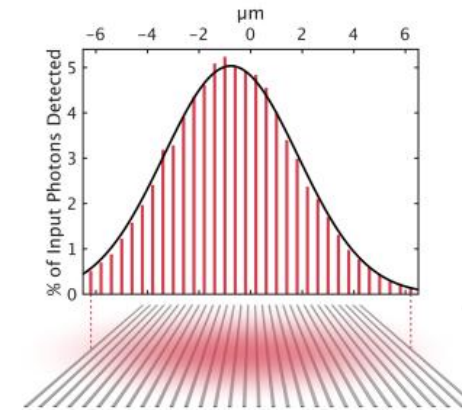
B. Korzh, *Nature Photonics* **14**, 250 (2020)

Large active area \rightarrow High efficiency \rightarrow High jitter, Low count rate

SNSPD Speed



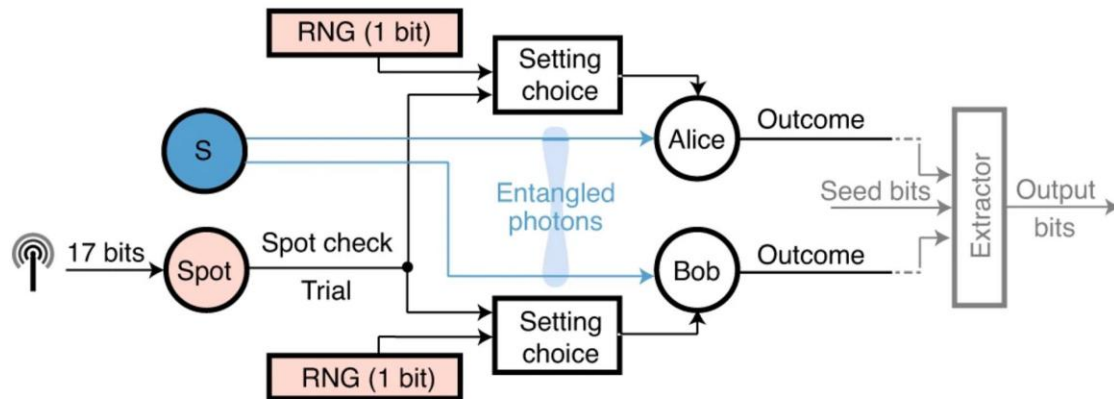
PEACOC array sampling SMF-28 optical fiber mode



Craiciu et al. (Optica 2023)

- Maximize count rate using multiple interleaved meanders; SNAP parallel readout
- Thermal relaxation of the hotspot: amorphous films (WSi, MoSi) $\sim 10\text{-}20$ ns ; NbTiN ~ 3 ns

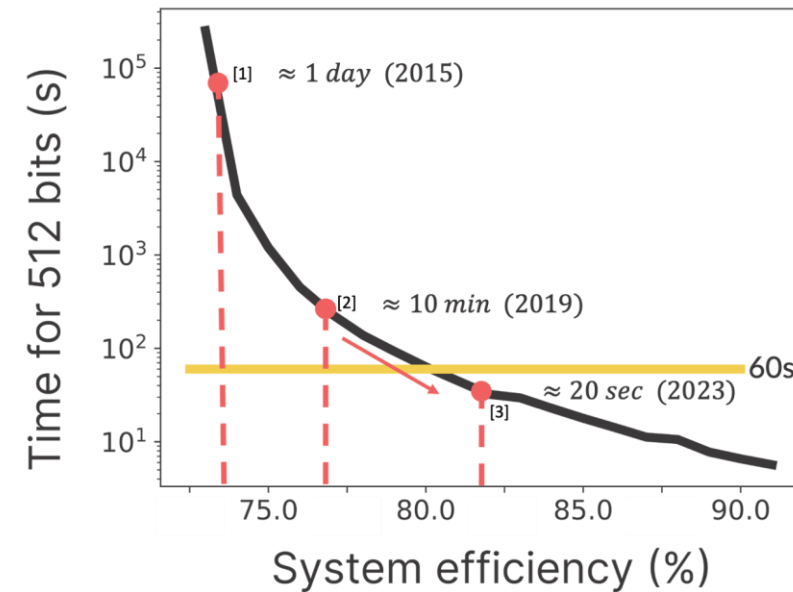
Randomness generation based on setup used in the loophole-free Bell violation experiment



(a)

Shalm, L.K *et al. Nat. Phys.* **17**, 452–456 (2021)

Kavuri, G.A., *et al. Nature* **642**, 916–921 (2025)



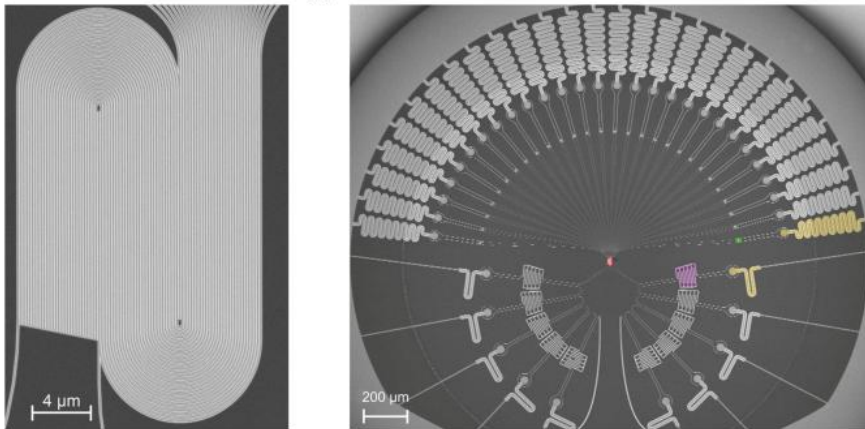
SNSPD QE ~ 98%
System entangled
pair-DE ~ 86%

- Measurements satisfy the conditions of a Bell test: the resulting bits are proven to be fundamentally random by Quantum mechanics
- Photon pair rate is kept low (PNR may reduce error rate slightly :limit double pair generation)
- Faster detectors : higher source rates (GHz)

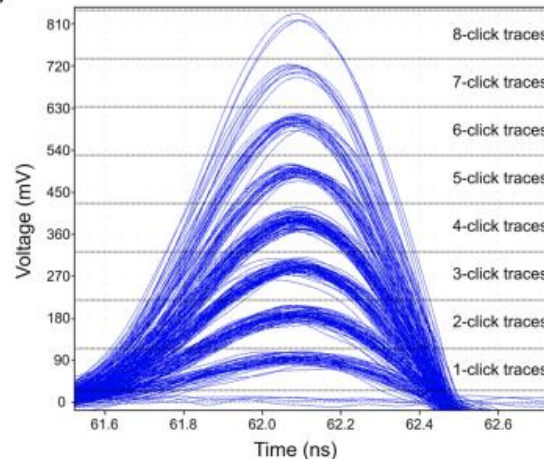
Quasi-Photon-Number Resolution

- Spatially multiplexed threshold detectors
- Approaches perfect PNR when the number of detectors is much larger than the number of photons

Parallel-SNSPD Architecture



Fast PNR discrimination up to 8 photons



SDE at 1550 nm :

1-photon efficiency 88%

2-photon efficiency 75%

3-photon efficiency 62%

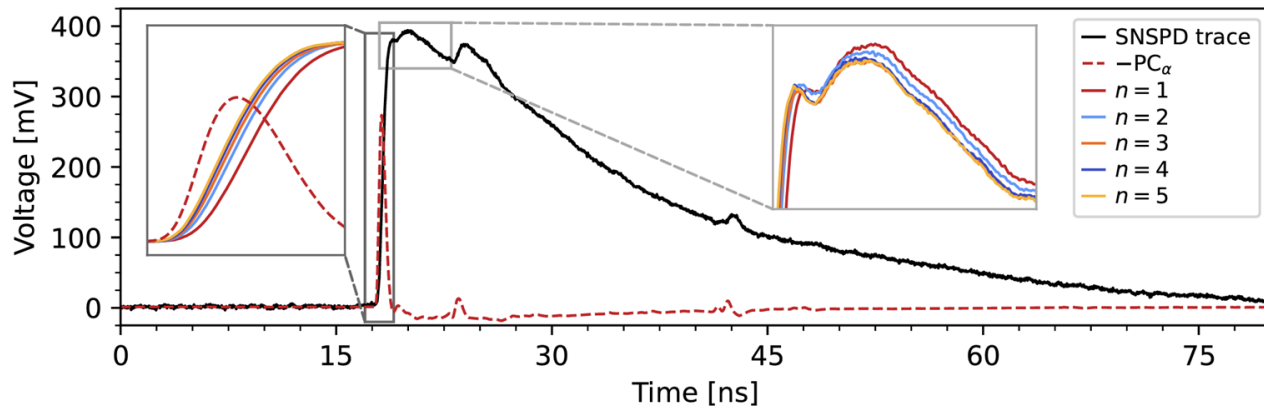
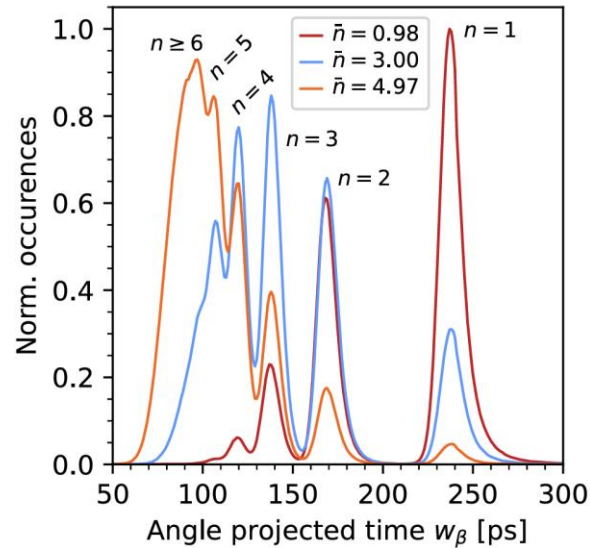
timing jitter < 80 ps

Speed 200 Mcps

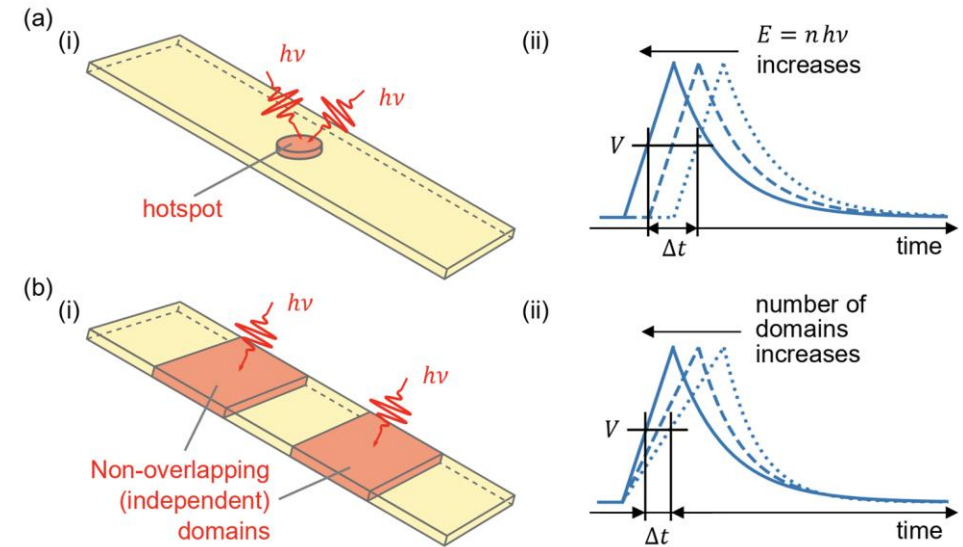
Stasi L. et al., : ACS Photonics 2025, 12, 320–329

Photon-number resolution with SNSPDs

- Pulse rising edge and amplitude contains PNR information
- Unambiguous discrimination between one- and two-photon events



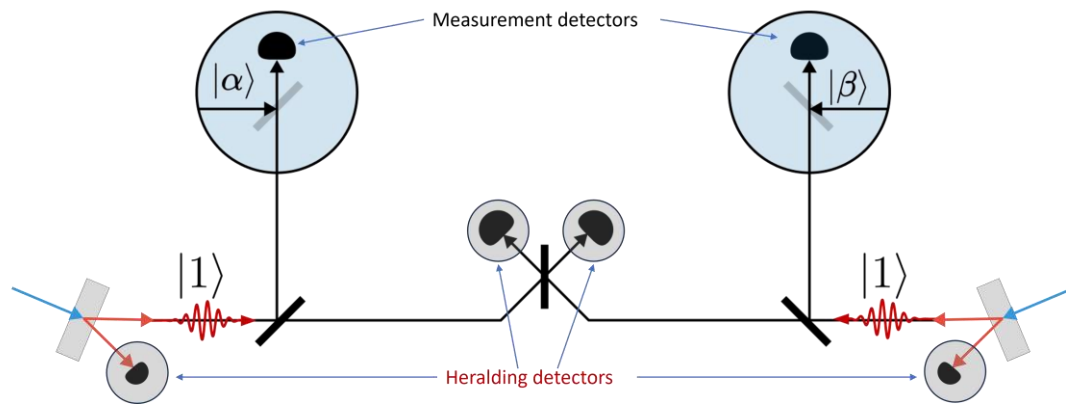
Schapeler T. et al., Phys. Rev. Applied 22, 014024 (2024)



Sidorova M. et al., APL Photon. 10, 086113 (2025)

Single-Photon Detectors for Quantum Networking

All-photonic path entanglement swapping

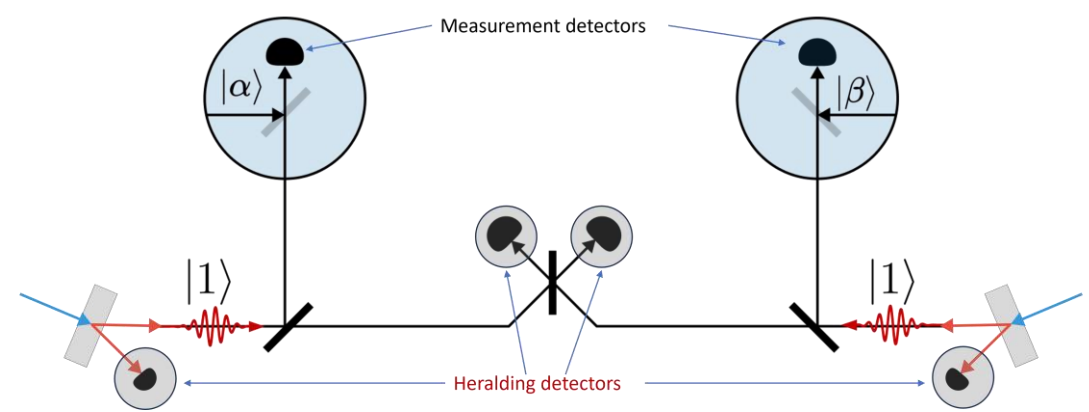


- Quantum communication protocol that entangles two independent photons that have never interacted, using only optical components and measurements
- Requires precise synchronization between pulses and so timing jitter can be a major limitation for distributing entangled photons

K. Shalm, MJ Stevens NIST

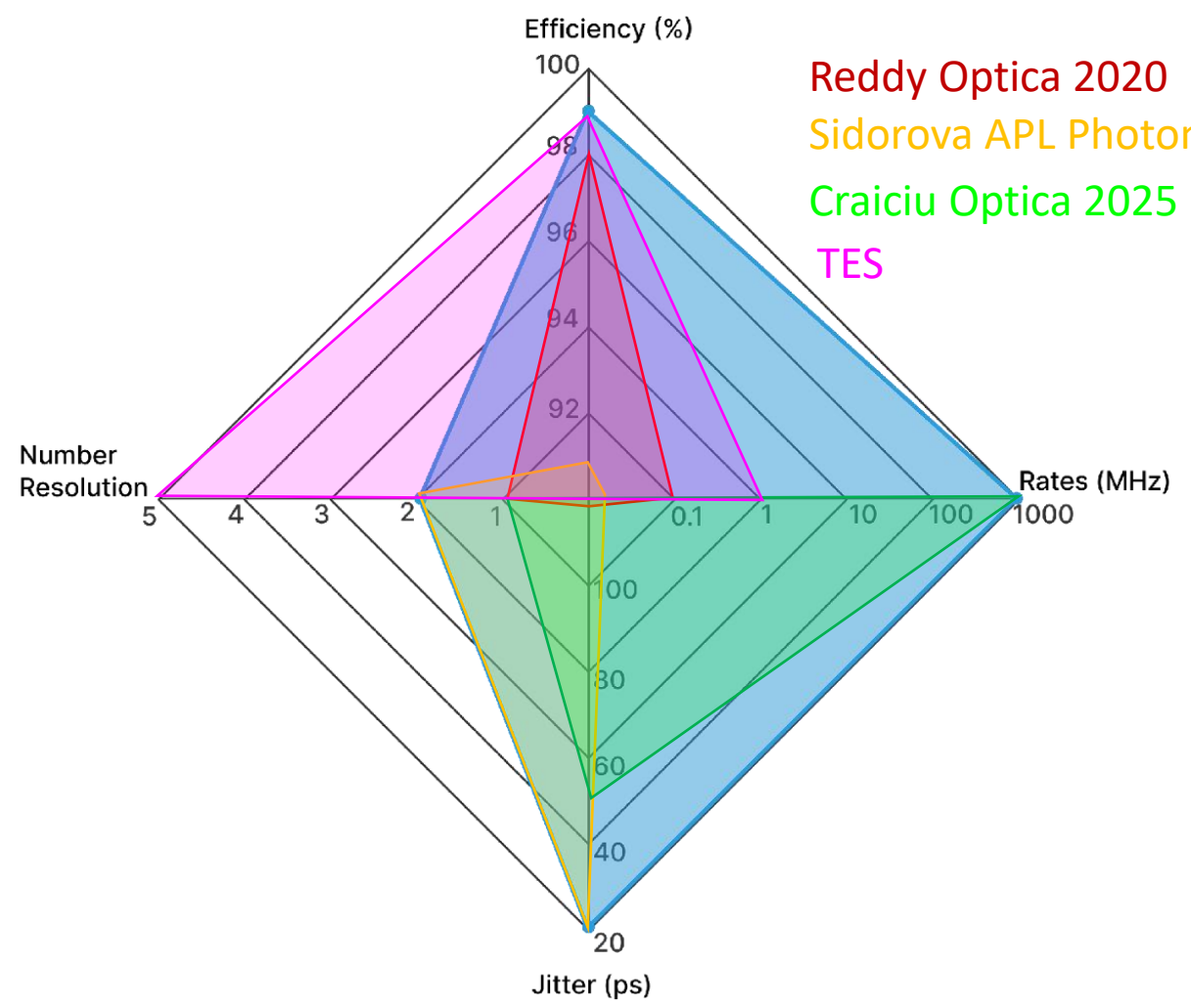
Single-Photon Detectors for Quantum Networking

All-photonic path entanglement swapping



K. Shalm, MJ Stevens NIST

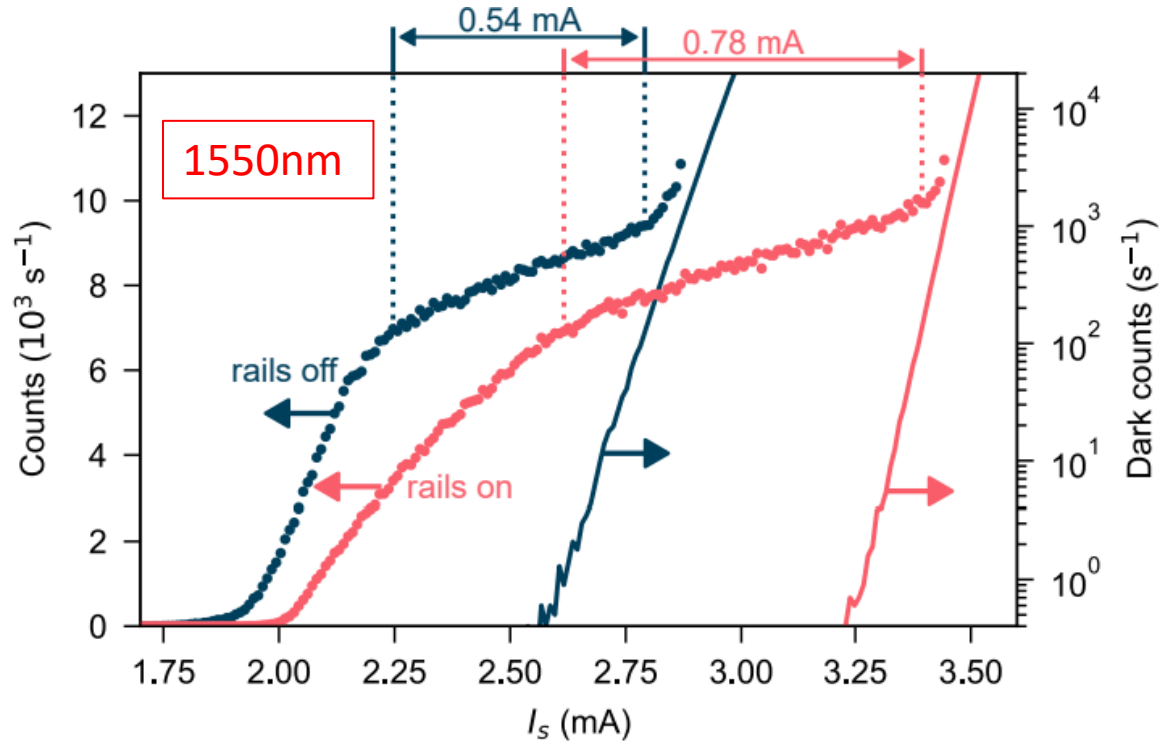
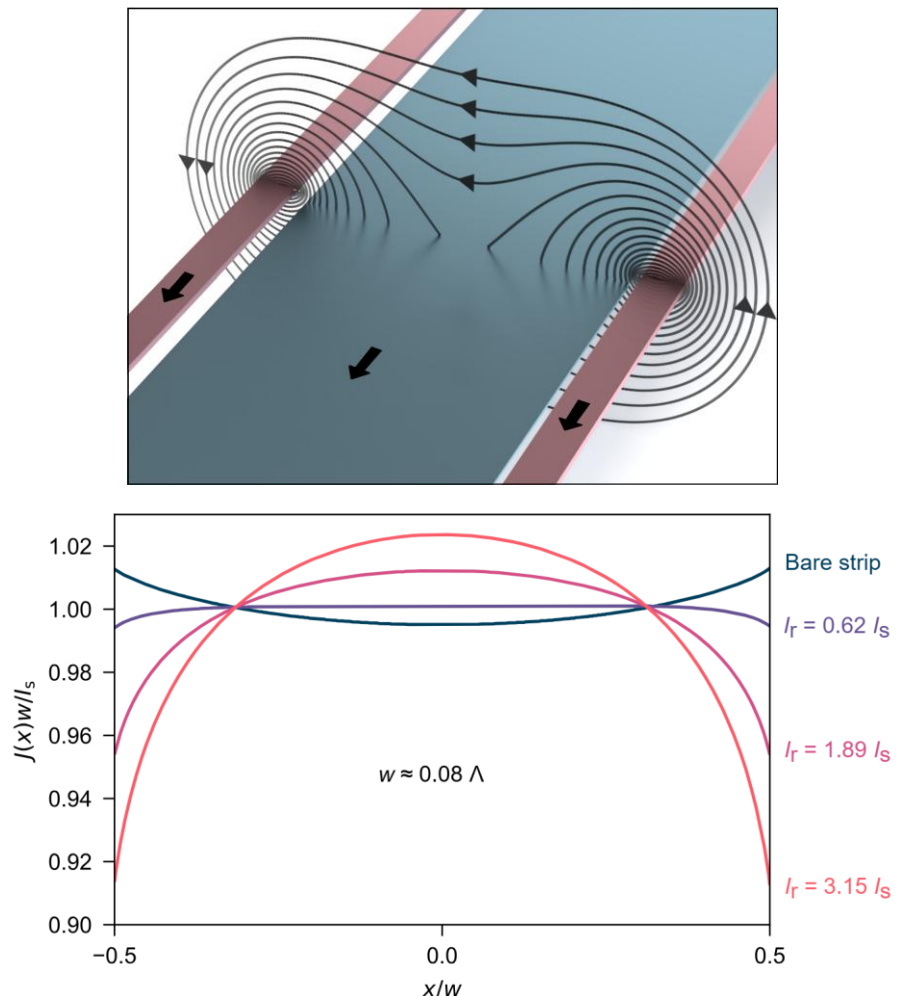
Heralding Detectors



Reddy Optica 2020
 Sidorova APL Photon.2025
 Craiciu Optica 2025
 TES

SNSPD Wide Wires

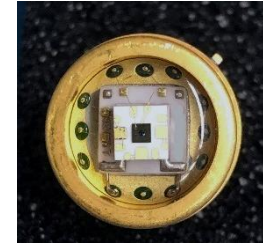
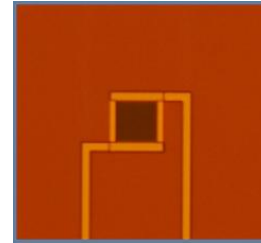
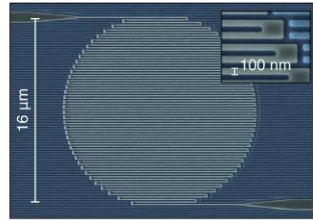
First demonstration of **0.1mm-wide** SNSPD!
 SNSPD-rail architecture pushes the detector to its performance limit



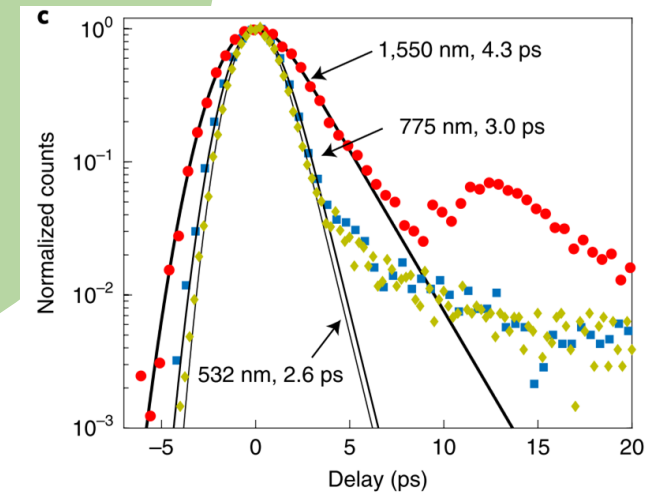
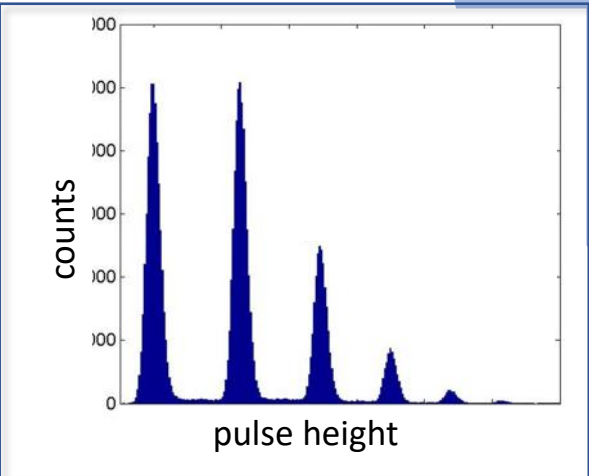
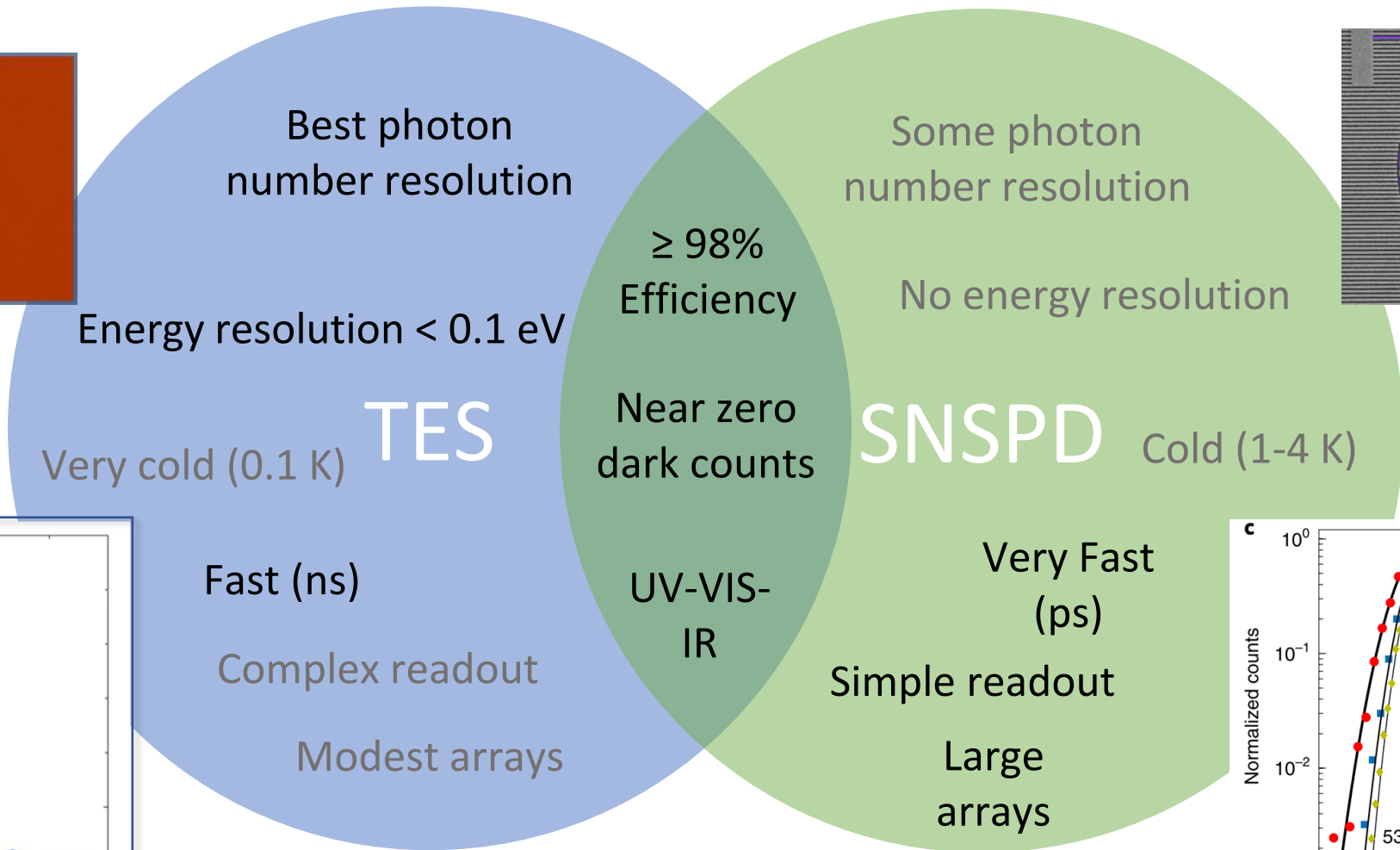
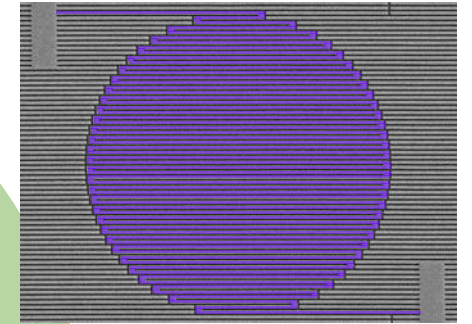
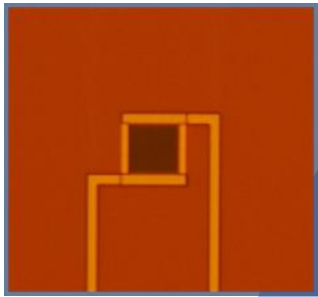
Parzuchowski, Kristen M., et al. *arXiv:2601.15971* (2026).

- Plateau length extended by > 40%
- Dark counts reduced by 10^{10}

Single-Photon Detectors



	SNSPD	TES	SPAD	PMT
Efficiency	$\geq 98 \%$	$\geq 98 \%$	85 % Si	$\leq 40 \%$
Energy Resolution	Some	Yes	Some	Yes
Recovery Time	10 ns	200 ns	10 ns	50 ns
Timing Jitter	< 10 ps	4 ns	20 ps	50 ps
Dark Counts	< 1 cnt/day	< 1 cnt/day	< 100 cps	< 200 cps
Wavelength Range	UV-MIR	UV-NIR	UV-NIR	UV-VIS
Operating Temperature	1-4 K	100 mK	RT	RT



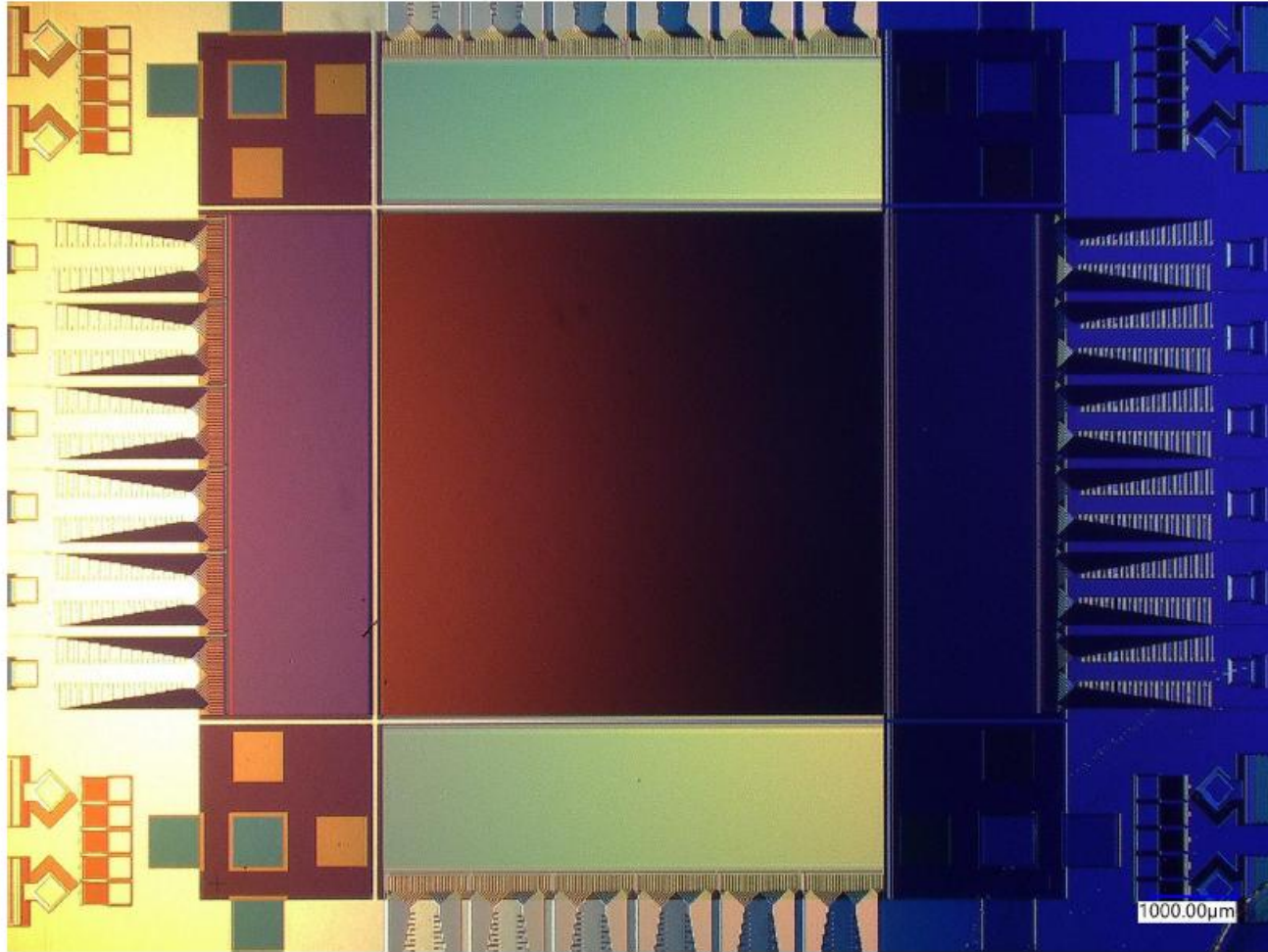
Faint Photonics & Quantum Nanophotonics



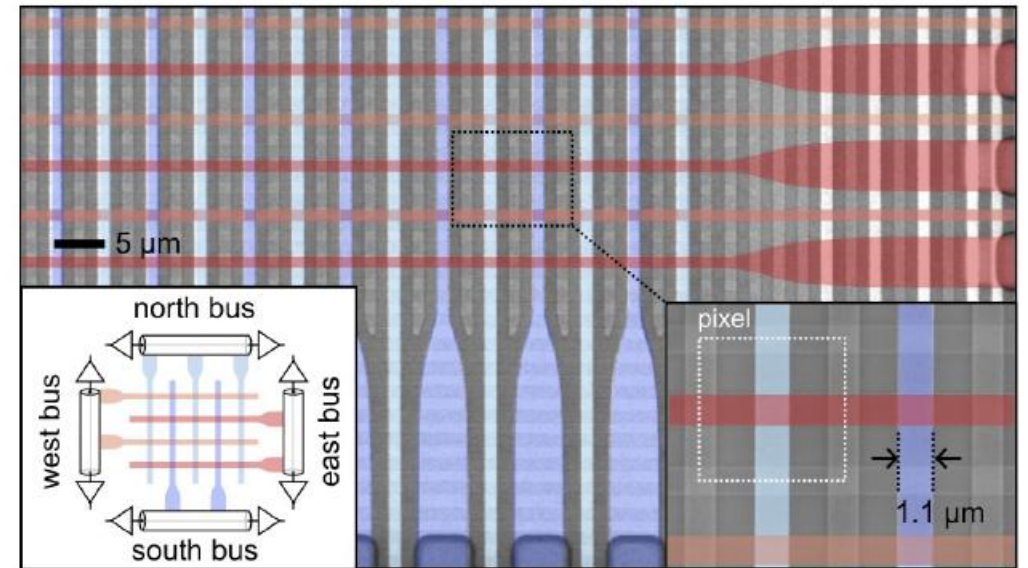
Sae Woo Nam
1970 - 2024



0.4 Megapixel SNSPD camera for Vis and Near-IR Imaging



- Array size: 800 x 500
- Active area: 4mm x 2.5mm
 - Pixel size: 5 μm x 5 μm
- Requires 8 coax
- Operated @ T = 0.8 K
- 0.13 cps dark counts across whole array



B.G. Oripov et al., *Nature* 622, 730–734 (2023).